DETERMINATION OF RESERVOIR AND WELL PARAMETERS BY ANALYZING THE PRESSURE SURVEY AND WELL TESTING DATA OF KAILASHTILLA, BIANY BAZAR AND RASHIDPUR GAS FIELDS

Md. Maksudur Rhman

DEPARTMENT OF PETROLEUM & MINERAL RESOURCES ENGINEERING
BANGLADESH UNIVERSITY OF ENGINEERING & TECHNOLOGY
DHAKA
BANGLADESH

APRIL, 2010

DETERMINATION OF RESERVOIR AND WELL PARAMETERS BY ANALYZING THE PRESSURE SURVEY AND WELL TESTING DATA OF KAILASHTILLA, BIANY BAZAR AND RASHIDPUR GAS FIELDS

A Project

Submitted to the Department of Petroleum and Mineral Resources Engineering in partial fulfillment of the requirements for the degree of Master of Engineering in Petroleum Engineering

By

Md. Maksudur Rhman

DEPARTMENT OF PETROLEUM & MINERAL RESOURCES ENGINEERING
BANGLADESH UNIVERSITY OF ENGINEERING & TECHNOLOGY
DHAKA
BANGLADESH

APRIL, 2010

RECOMMENDATION OF THE BOARD OF EXAM

The undersigned certify that they have read and recommended to the Department of Petroleum and Mineral Resources Engineering for acceptance, a project entitled "**Determination of Reservoir and well Parameters by Analyzing the Pressure Survey and Well Testing Data of Kailashtilla, Biany Bazar and Rashidpur Gas Fields.**" submitted by **MD. MAKSUDUR RAHMAN** in partial fulfillment of the requirements for the degree of **MASTER OF ENGINEERING IN PETROLEUM ENGINEERING** on 3rd April, 2010.

Chairman (Supervisor) : _____

Dr. Mahbubur Rahman
Assistant Professor
Department of PMRE, BUET, Dhaka.

Member : _____

Dr. Mohammad Tamim
Professor and Head
Department of PMRE, BUET, Dhaka.

Member (External) : _____

Mr. Zaved Choudhury
Director,
Energy Regulatory Commission
Karwanbazar C/A, Dhaka -1215.

DECLARATION

It is hereby declared that this project or any part of it has not been submitted elsewhere for the award of any degree or diploma.

.....

(Md. Maksudur Rhman)

Abstract

Well testing provides reliable information about the reservoir and the producing wells that produce from that reservoir. Main reservoir parameters, total permeability-thickness product, kh (md. ft), average permeability, K (md) and initial reservoir pressure, Pi (Psia), and well parameters such as wellborstorage coefficient, C (bbl/psi) and skin, S, are estimated in this project work by using well testing software package (Well Test by Fekete associates Inc.).

Data were collected from 8 (eight) wells, 3 (three) of Kailastilla Gas Field, 2 (two) of Biany Bazar Gas Field, 3 (three) of Rasidpur Gas Field, operating under Sylhet Gas Field Limited (SGFL), a company of Petrobangla. Same data are analyzed by Almansoori Wireline Services, a third party welltesting service provider. Intercomp-kanata Management Ltd. (IKM), Oil & Gas Field Exploration Services Company, also determined these reservoir and well parameters under a contract with Petrobangla. The results of the analysis of this project work, AL Mansoori Wireline Services and IKM are shown in a table at the end of the diagnosis of each well.

The synthetic pressure and pressure derivative data match with actual pressure and pressure derivative plots, Absolute Open Flow (AOF), coefficient, C, and exponent, n, of the deliverability equation are estimated through this thesis work. The main parameters average permeability, K (md), and skin, S, for KTL#1, KTL#2, KTL#4, BB#1, BB#2, R#1, R#4 and R#7 are 134 and 2.4, 5575 and 4.1, 238 and 9.8, 213 and 17.1, 95.6 and 13.8, 2150 and 7.2, 16 and -4.8, 20.8 and -0.70 respectively. However, from core data analysis; Average Permeability of the Middle Gas Sand, producing zone of KTL#1 and KTL#4, of Kailastilla Gas Field is 88.4 md, and 424.3 md for the Upper Gas Sand, producing zone of KTL#2, of Kailastilla Gas Field, Average Permeability of the Lower Gas Sand, producing zone of BB#1, of Biany Bazar Gas Field is 189.6 md, and 332.4 md for the Upper Gas Sand, producing zone of BB#2, of Biany Bazar Gas Field, and Average Permeability of the Upper Gas Sand, producing zone of R#1, R#4 and R#7, of Rasidpur Gas Field is 370.0 md.

Acknowledgments

First and foremost, I would like to thank my advisor, Dr. Mahbubur Rahman, for his constant support and guidance during this study. I would like to express my sincere gratitude for his patience and encouragement throughout this work, without which this work would not have been possible.

I am extremely grateful to Prof. Dr. M. Tamim for his valuable insightful ideas, advice, help and supervision in different stage of this work.

I am extremely grateful to Mr. Javed Chowdhury, Director, Energy Regulatory Commission, for his valuable suggestions.

Special thanks also go to Sylhey Gas Field Limited (SGFL) for their support and provide data for our research efforts.

I would also like to thank all my friends and colleagues for their consistent support during my research efforts.

Table of Contents

List of Figures

FIGURE Page

List of Tables

Nomenclature

A	Reservoir drainage area, ft^2
AOF	Absolute open flow potential
B	Formation volume factor, reservoir bbl/stock tank bbl
C	Performance Coefficient
C_A	Shape factor
c_f	Formation (rock) compressibility, psi^{-1}
c_g	Gas compressibility, psi^{-1}
c_t	Total system compressibility, psi^{-1}
c_w	Water compressibility, psi^{-1}
h	Reservoir (net pay) thickness, ft
IKM	Intercomp-Kanata Management Ltd.
k	Formation permeability, md
m	semilog slope $(=162.6Bm/kh)$, psi/log-cycle
m(p)	Real gas pseudopressure, $psia^2/cp$
n	Exponent
$\overline{p}$	Average reservoir pressure, psia
p_D	Dimensionless, pressure, dim-less
p_i	Initial reservoir pressure, psia
$\overline{p}_R$	Average reservoir pressure
p_{wf}	Flowing sandface pressure, psia
p_{ws}	Shut-in pressure
q	Production rate, MMscfd or bbl/d
q_D	Dimensionless production rate
q_g	Gas flowrate, MSCF/D
r	Distance from wellbore
r_{eD}	Dimensionless reservoir radius, dim-less
r_e	Reservoir drainage radius, ft
r_w	Wellbore radius, ft
s	Skin factor
t	Time, hr
t_{ca}	Material-balance-pseudo-time, days
t_D	Dimensionless time
t_{DA}	Dimensionless time based on area
T_R	reservoir temperature, deg R (T is also given in deg F, but deg R is used in calculations)
z	Gas compressibility factor

Subscripts:

avg	Average
D	Dimensionless
g	Gas
o	Oil
i	Initial condition
k	well position index
p	Pseudoperssure
wf	Wellbore flowing conditions

Greek Symbols:

Δ	Finite change
j	Derivative
f	Porosity, fraction
y	Pseudo-pressure
y_{wf}	Following Pseudo-pressure
g	0.577216, Euler's constant
m	Fluid viscosity, cp

CHAPTER 1

Introduction

Well testing is one of the most useful aids to provide reliable information about the reservoir and the producing wells that produce from that reservoir. Moreover, the ability to analyze the performance and forecast the productivity of wells and to understand the behavior of reservoirs with a reasonable degree of accuracy is of utmost importance in today's oil and gas industry. A complete analysis and understanding of the results of an appropriate well test enables one to determine the stabilized shut-in reservoir pressure (Theis,1935; Horner,1951; Ramy,1971) and the rate at which a well will flow against a particular pipe-line "back pressure" (Rawlins and Schellhardt 1936). It also enables one to predict the manner in which the flow rate will decrease with depletion and the resulting decline in reservoir pressure, and estimate the effective flow characteristics (Carslaw and Jaeger, 1959; Bear, 1972).

Sylhet Gas Field Limited (SGFL), a company of Petrobangla, is the pioneer of energy sector in Bangladesh. Haripur, operating under SGFL, is the oldest gas field in Bangladesh. In 1957, gas production started from Haripur Gas field at the first time from the history of the then East Pakistan. In course of time, number of wells and gas fields are increased to fulfill expanding country demand. At present, SGFL operates four Gas Fields –1) Haripur Gas Field, 2) Rasidpur Gas Field, 3) Kailastilla Gas Field, and 4) Biany Bazar Gas Field. As reservoirs are depleted, producing wells show decreasing pressure trend. Some wells have been abandoned already and some wells exhibit abnormal pressure behavior (SGFL Annual Report 2006-07). It is, therefore, very important to assess correctly the existing reserves and evaluate the production performance of the producing wells. SGFL-management decided to determine reservoir properties and well condition through well testing. Pressure Survey program was undertaken all producing wells of all the four gas fields under SGFL. The complete job, i.e. data collection and interpretation, was performed by a third party contractor specialized for this type of work.

It is important to develop in-house and local expertise to carry out this type of work. The data collection part involves special equipment and procedures, which are not currently available within the state-run companies. Once the data is obtained, however, interpretation can be exercised by using the computers and software, following well-established procedures. This project aims to analyze the data, independent of the contractor, to gain

understanding of the reservoir-well system. It should provide an opportunity to compare the findings of the contractor. It should also help the local industry building confidence and expertise in this very challenging domain of reservoir engineering.

Objective with specific aims and possible outcome:

The objective of the study has subdivided as follows:

1. Determine the formation permeability (k) and completion characteristic (skin, s) of each well.
2. Determine any reservoir barriers to flow in the vicinity of the well.
3. Determine current reservoir pressure, temperature, etc.
4. Determine productivity of the formation and well deliverability.

Methodology outline:

To achieve the above objectives the following methods are adopted:

1. Study the theories and current practice of Well Testing;
   1.1. Conventional Back Pressure test;
   1.2. Build-up and Draw down test;
2. Collect well test data;
3. Analyze well test data by hand calculations, spreadsheet and by well testing software package (Well Test by Fekete associates Inc.).

CHAPTER 2

Literature Review

During a well test, the response of a reservoir to changing production (or injection) conditions is monitored. Since the response is to a greater or lesser degree characteristic of the properties of the reservoir, it is possible in many cases to infer reservoir properties form the response. In most cases of well testing, the reservoir response that is measured is the pressure response. Hence in many cases well test analyses is synonymous with pressure transient analysis. The pressure transient is due to changes in production or injection of fluids, hence we treat the flow rate transient as input and the pressure transient as output. In well test interpretation, we use a mathematical model to relate pressure response (output) to flow rate history (input). In most cases, the design and the interpretation of a well test is dependent on its objectives. The objectives of a well test usually fall into three major categories:

1. Reservoir evaluation,
2. Reservoir management, and
3. Reservoir description.

Types of tests

Basically, there are tow types of flow tests conducted on wells. The first category involves tests designed primarily to measure the deliverability of wells and the second category involves tests designed primarily to yield knowledge of the reservoir. The conventional back pressure test and the isochronal type tests are examples of tests designed primarily to measure deliverability. These types of tests are described in chapter 5. Tests designed primarily to yield knowledge of the reservoir can be further categorized as drawdown tests and build-up test which are described in the later section of this chapter. Other common types of tests are Injection Test, Falloff Test, Interference Test, and Drill Stem Test (DST).

The various types of test are defined in the following section.

Drawdown Test

In a drawdown test, a well that is static, stable and shut-in is opened to flow. For the purposes of traditional analysis, the flow rate is supposed to be constant (Figure 2.1).

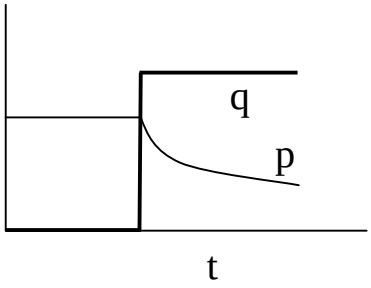

Figure 2.1: p-q-t diagram of drawdown test

Buildup Test

In a buildup test, a well which is already flowing (ideally at constant rate) is shut in, and the downhole pressure measured as the pressure builds up (fig. 2.2). Analysis of a buildup test often requires only slight modification of the techniques used to interpret constant rate drawdown test. The practical advantage of a buildup test is that the constant flow rate condition is more easily achieved (since the flow rate is zero).

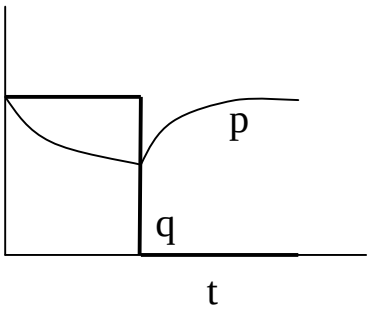

Figure 2.2: p-q-t diagram of build-up test

Injection Test

An injection test is conceptually identical to a drawdown test, except that flow is into the well rather than out of it (fig. 2.3). Injection rates can often be controlled more easily than production rates, however analysis of the test results can be complicated by multiphase effects unless the injected fluid is the same as the original reservoir fluid.

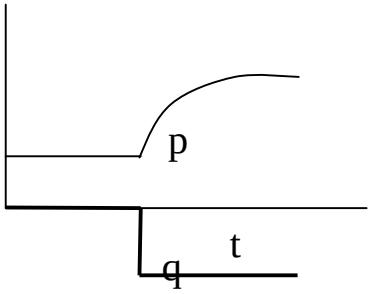

Figure 2.3: p-q-t diagram of Injection Test

Falloff Test

A falloff test measures the pressure decline subsequent to the closure of a injection (fig. 2.4). It is conceptually identical to a buildup test. As with injection tests, falloff test interpretation is more difficult if the injected fluid is different from the original reservoir fluid.

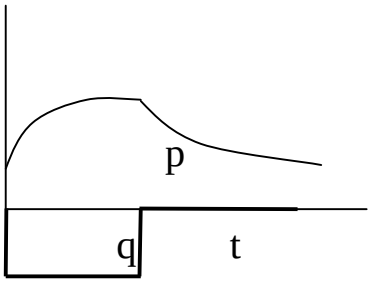

Figure 2.4: p-q-t diagram of Falloff Test

Interference Test

In a interference test, one well is produced and pressure is observed in different well (or wells). An interference test monitors pressure changes out in the reservoir, at a distance from the original producing well. Thus an interference test may be useful to characterize reservoir properties over a greater length scale than single-well tests. Pressure changes at a distance from the producer are very much smaller than in the producing well itself, so interference tests require sensitive pressure recorders and may take a long time to carry out. Interference tests can be used regardless of the type of pressure change induced at the active well (drawdown buildup, injection or falloff).

Drill Stem Test (DST)

A drill stem test is a test which uses a special tool mounted on the end of the drill string. It is a test commonly used to test a newly drilled well, since it can only be carried out while a rig is over the hole. In a DST, the well is opened to flow by a valve at the base of the test tool, and reservoir fluid flows up the drill string (which is usually empty to start with). A common test sequence is to produce, shut in, produce again and shut in again. Drill stem tests can be quite short, since the positive closure of the downhole valve avoids wellbore storage effects. Analysis of the DST requires special techniques, since the flow rate is not constant as the fluid level rises in the drill string. Complications may also arise due to momentum and completion operations may influence the results.

Basic Fluid-Flow Equation

The differential equation for fluid flow in a porous medium, the diffusivity equation, is a combination of the law of conservation of matter, an equation of state, and Darcy's law. When expressed in redial coordinates, the diffusivity equation is

$$\frac{\partial^2 p}{\partial r^2}+\frac{1}{r}\frac{\partial p}{\partial r}=\frac{1}{0.0002637}\frac{fmc_t}{k}\frac{\partial p}{\partial t} \quad \text{.....(2.1)}$$

Matthews and Russell (1967) present a derivation of Eq. 2.1 and point out that it assumes horizontal flow, negligible gravity effects, a homogeneous and isotropic porous medium, a single fluid of small and constant compressibility, and applicability of Darcy's law and that $m, c_t, k \text{ and } f$ are independent of pressure.

Dimensionless Variables

Well Test analysis often makes use of dimensionless variables. The importance of dimensionless variables is that they simplify the reservoir the models by embodying the reservoir parameters (such as k), thereby reducing the total number of unknowns. They have the additional advantage of providing model solutions that are independent of any particular unit system. It is an inherent assumption in the definition that permeability, viscosity, compressibility, porosity, formation volume factor and thickness are all constant.

The dimensionless pressure p_D is defined (in oilfield units) as:

$$p_D = \frac{kh}{141.2qBm}(p_i - p_{wf}) \quad \text{.....(2.2)}$$

where:

k	=	permeability (md)
h	=	thickness (feet)
p_i	=	initial reservoir pressure (psi)
p_{wf}	=	well flowing pressure (psi)
q	=	production rate (STB/d)
B	=	formation volume factor (res vol/std vol)
m	=	viscosity (cp)

In a consistent unit set, p_D is defined as:

$$p_D = \frac{2pkh}{qBp}(p_i - p_{wf})$$

The dimensionless time t_D is defined (in oilfield units) as:

$$t_D = \frac{0.000264kt}{fmc_t r_w^2} \quad \text{.....(2.3)}$$

where:

t	=	time (hours)
f	=	porosity (pore volume/bulk volume)
c_t	=	total system compressibility (/psi)
r_w	=	wellbore radius (ft)

In a consistent unit set, p_D is defined as:

$$t_D = \frac{kt}{fmc_t r_w^2}$$

This is only one form of the dimensionless time. Another definition in common usage is t_{DA}, the dimensionless time based upon reservoir area:

$$t_{DA} = \frac{kt}{fmc_t A}$$

where:

A = reservoir area = $p\ r_e^2$

r_e = reservoir radius (ft)

Clearly there is direct relationship between t_D and t_{DA}:

$$t_D = t_{DA}\frac{A}{r_w^2} = t_{DA}p\,\frac{r_e^2}{r_w^2}$$

We can also define a dimensionless radius, r_D, as:

$$r_D = \frac{r}{r_w} \qquad \text{.....(2.4)}$$

This definition is independent of any particular set of units.

Dimensionless Pressure during the Infinite-Acting Flow Period:

Intermediate time response, between the early wellbore-dominated response and the late time boundary-dominated response, is known as the infinite acting period.

The exponential-integral solution (also called the line source or the Theis (1935) Solution) of equation (2.1) with boundary conditions

a. $p = p_i$ at t = 0, for all r

b. $p = p_i$ at r= ∞, for all t

c. $\lim_{r\to 0}\left(r\frac{\partial p}{\partial r}\right) = \frac{qm}{2pkh}p_i$, for t > 0

Condition c. is the line source inner boundary condition

is

$$p_d\left(t_{D,r_D}\right) = -\frac{1}{2}Ei\left(\frac{-r_D^2}{4t_D}\right) \qquad \text{.....(2.5}a\text{)}$$

$$\cong \frac{1}{2}\left[1n(t_D/r_D^2) + 0.80907\right] \qquad \text{.....(2.5}b\text{)}$$

Eq. 2.5b may be used when

$t_D/r_D^2 > 100,$ .....(2.6)

Dimensionless Pressure during the Pseudosteady-State Flow Period

Pseudo-Steady State (PSS) flow occurs during the late time region when the outer boundaries of the reservoir are all no-flow boundaries. This includes not only the case when the reservoir boundaries are sealing faults, but also when nearby producing wells cause no-flow boundaries to arise. During the PSS flow regime, the reservoir behaves as a tank. The pressure throughout the reservoir decreases at the same, constant rate. PSS flow does not occur during build-up or falloff tests.

During pseudosteady state, dimensionless pressure is given by Ramey and Cobb (1971) with the boundary condition: $dp/dt =$ constant for all r (that is equivalent to the right-hand side of equation. (2.1) being constant).

$$p_d = 2pt_{DA} + \frac{1}{2}1n\left(\frac{A}{r_w^2}\right) + \frac{1}{2}1n\left(\frac{2.2458}{C_A}\right) \quad \text{.....(2.7)}$$

$C_{A,}$ the shape factor, is a geometric factor characteristic of the system shape and the well location. Values are given by Brons and Miller (1961), Dietz (1965) and others.

Steady State Flow

Steady State flow occurs during the late time region when a constant pressure boundary exists. Constant pressure boundaries arise when the reservoir has aquifer support or gas cap expansion support.

When the pressure at every point in a system does not vary with time i.e. $dp/dt = 0$ (that is, when the right-hand side of Eq. 2.1 is zero), flow is said to be steady state. The dimensionless-pressure functions are

steady state, linear

$$(p_D)_{ssL} = 2p\frac{Lh}{A}, \quad \text{.....(2.8)}$$

steady state, redial

$$(p_D)_{ssr} = 1n\left(\frac{r_e}{r_m}\right) \quad \text{.....(2.9)}$$

Application of Flow Equation to Gas Systems

Gas viscosity and density vary significantly with pressure, so the assumptions of equation 2.1 are not satisfied for gas systems and the equation does not directly to gas flow in porous media. That difficulty is avoided by defining a "real gas potential" byAl-Hussainy (1966), also commonly referred to as the real gas pseudopressure or just pseudopressure, and "pseudotime" by Agarwall(1979).

Pseudopressure

The real gas pseudopressure is defined as

$$m(p) = \Psi = 2\int_{p_b}^{p} \frac{p}{mz} dp \qquad (2.10)$$

Pseudotime

Agarwall's pseudotime is defined as

$$t_a = \int_0^t \frac{1}{mc_t} dt \qquad (2.11)$$

2.1 Drawdown Testing

Important reservoir parameters can be determined by flowing a well at a constant rate and measuring flowing wellbore pressure as a function of time. This is called drawdown testing and it can utilize information obtained in both the transient and pseudo-steady-state flow regimes. If the flow extends to the pseudo-steady state, the test is referred to as a reservoir limit test and can be used to estimate in-place gas and shape of the reservoir. Both single-rate and multi-rate tests are utilized depending on the information required. The purpose of the drawdown testing is to determine the reservoir characteristics that will affect flow performance. Some of the important characteristics are the flow capacity kh, skin factor s, and turbulence coefficient D.

In the absence of wellbore storage and skin effects, the pressure transient due to infinite acting radial flow into a line source wellbore producing at constant flow rate is given by equation 2.5b. Writing this equation in dimensional variables including skin effects, we get

$$p_{wf} = p_i - 162.6\frac{qB\mu}{kh}\left(\log t + \log\frac{k}{f\mu c_1 r_w^2} + 0.8686s - 3.2274\right) \quad \text{.....(2.12)}$$

where the natural logarithm (In) has been replaced by logarithm to base 10 (log). From this equation it is seen that a plot of pressure drop against the logarithm of time should contain a straight line, called semilog straight line, with slope:

$$m = 162.6\frac{qB\mu}{kh} \quad \text{.....(2.13)}$$

Hence the recognition of this slope makes it possible to estimate the permeability (k) or the permeability-thickness product (kh), also known as conductivity of the porous media. Many traditional well test interpretation techniques are based on this "semilog approach" and the recognition of the correct semilog straight line is a crucial aspect of this type of analysis

The skin factor can be estimated from the difference between pi and the intercept of the staight line. This can be done conveniently by substituting the time 1 hour in Eq. (2.12) and solving for s

$$s = 1.151\left[\frac{p_i - p_{1hr}}{m} - \log\frac{k}{f\mu c_1 r_w^2} + 3.2274\right] \quad \text{.....(2.14)}$$

It is important to note that the value of p_{1hr} needs to be taken from the straight line, or the extrapolation of it. This is due to the assumption of infinite acting radial flow- -the flow regime at the arbitrary time of 1 hour may not be infinite-acting, and therefore the actual pressure data point at this time is not the correct one to use.

Semilog Analysis

Semilog analysis is based on the location and interpretation of the semilog straight line response (infinite acting radial flow). However, it is very important to note that semilog analysis is not based on the semilog straight line alone, since it is first necessary to determine, based on the duration of the wellbore storage effect, the time at which the semilog straight line begins. Not all well tests will necessarily include an infinite acting radial flow response period, and an apparent straight line on a semilog plot may not in itself be representative of radial flow. Therefore it is always important to begin a semilog analysis by considering the storage effect, to gain confidence in locating the semilog straight line correctly.

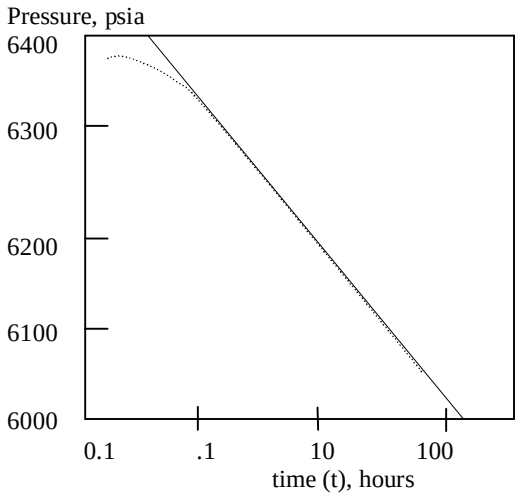

Figure 2.5: Semilog straight line for drawdown test

The wellore storage shows as a unit slope straight line on a log-log plot of p vs. t. There is about 1½ log cycles between the end of the unit slope straight line representing wellbore storage and the start of the purely reservoir response (infinite acting radial flow in cases of

interest in the context of semilog analysis). This observation gives rise to the 1½ log cycle rule, providing us with a useful method of identifying the start of the semilog straight line.

Hence the steps involved in a simple semilog analysis are:

1. Drawing a log-log plot of p vs. t
2. Determination the time at which the unit slope line ends
3. Noting the time 1½ log cycles ahead of that point, this is the time at which the semilog straight line can be expected to start
4. Drawing a semilog plot of p vs. t
5. Looking for the straight line, starting at the suggested time point
6. Estimation of the permeability, k, from the slope of the straight line, using Eq. (2.13)
7. Estimation of the skin factor, s, from the intercept of the line, using the pressure
8. point at t=1 hour on the straight line (not on the data) and Eq. (2.14).

2.2 Build-Up Testing

The primary purpose of performing a build-up test is to determine the well-bore damage (skin) and the reservoir permeability. However, during the course of a build-up, it is possible to encounter reservoir boundaries. If all the reservoir's boundaries are contacted during the build-up, the size of the reservoir can also be determined. If the well has been pressure tested before, subsequent testing allows relative material balance calculations (decline curve analysis), as well as the determination of the drive mechanism for the reservoir.

Operationally, pressure build-up tests are simplest of all gas well tests. The field conduct of such tests essentially involves a shut-in of the wellbeing tested and subsequently monitoring the build-up of the bottom hole/wellhead pressure. Because of the absence of operational problems which are frequently associated with drawdown tests, like maintaining constant flow rates or preventing hydration in flow lines, a build-up test, properly conduced and interpreted, will usually give the most dependable results.

Build-up tests are often conducted as part of an annual pressure survey of pool. The average pressure, resulting from a build-up analysis, reflects the remaining reserves. In high permeability reservoirs the pressure will build up to a stabilized value quickly, but in tight formations, the pressure may continue to build up for months before stabilization is attained. Loss of production during a long shut-in may be intolerable economically. However, prohibitively long shut-in periods may be avoided when a proper analysis f the transient pressure-time data is possible. Such an analysis yields values of permeability, k, apparent skin factor, s', and the average reservoir pressure, $\overline{P}_R$.

There are a few publications that form the core of pressure build-up analyses. These have resulted in three conventional methods of analysis, namely, the Horner plot, the Miller-Dyes-Hutchinson (MDH) plot and the Muskat plot.

Theis (1935), and later Horner (1951), showed that a plot of the shut-in pressure, P_{WS}, versus log $(t+ \Delta t/\Delta t)$ would result in a straight line for an infinite-acting reservoir. In the context of build-up tests, t refers to the drawdown period prior to a build-up and Δt refers to the shut-in or build-up time. Matthews, Brons and Hazebroek (MBH) (1954), extended the application of the Horner plot to finite reservoirs.

Miller-Dyes-Hutchinson (1950), and subsequently Perrine (1956), showed that if a well has been produced to pseudo-steady state flow conditions and then shut in, a plot of the shut-in pressure, P_{WS}, versus log Δt will give a straight line.

Muskat (1936), Larson (1963) and Russell (1966) stated that a plot of log ($\overline{P}_R$ - P_{WS}) versus Δt would, under certain circumstances, give a straight line.

In the conduct and analysis of build-up tests, it is very bear in mind a build-up is always preceded by a drawdown, and also that the build-up data are directed affected by this drawdown. Ideally, the drawdown starts from a stabilized reservoir pressure, p_i. At a time, t, the well is shut-in and the build-up is continued for a time, Δt.

In pressure transient analysis a reservoir is idealized by making the assumptions of equation (2.1). Under these conditions, the behavior of the static sand face pressure, $P_{ws,}$ is depicted in figure 2.6.

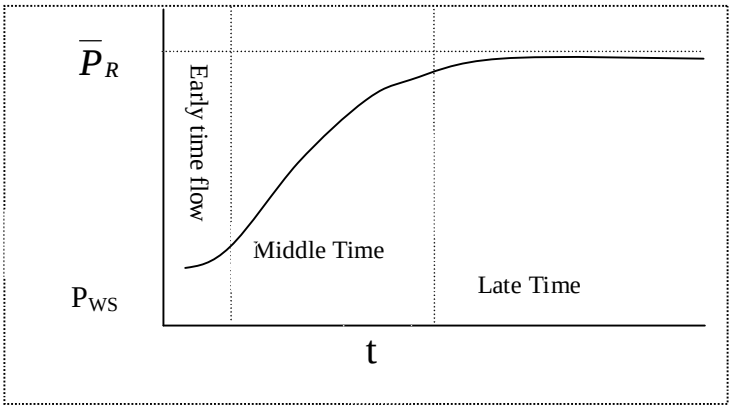

Figure 2.6: Behavior of the static sand face pressure upon shut-in of a well

The early-time portion reflects the wellbore storage (after flow) and apparent skin effects. Wellbore storage results from closing the well at the surface instead of at the sand face. Production continues from the formation into the wellbore for some time after the flow at the surface has been stopped. In low-permeability gas-condensate reservoirs, wellbore storage should be avoided and it is usually imperative to use a bottom hole shut-in tool (Dykstra, 1961). Skin effects results from wellbore damage, the nature of completion of the well and from IT flow.

The data that fall in the middle-time region constitute the most useful part of abuild-up test. The previously mentioned plots, Horner-MBH, and the MDH, utilize these data to obtain a straight line plot on semilogarithmic coordinate graph paper. The permeability thickness, kh, deduced from these semilog straight lines. Early-time data must be excluded from such plots. Wattenbarger and Ramey (1968) investigated the effects of turbulence, well damage, and wellbore storage and in every case found that the proper straight line was obtain following early-time deviations.

Late-time data are usually marked by a deviation from the semilog straight line of the middle-time region. This deviation reflects the effects of boundaries. If the shut-in period is sufficiently long, the final pressure attained, called the stabilized shut-in pressure, is infact the average pressure of the reservoir volume being drained.

Conceptually, a build-up is treated as the result of two superposed effects, shown in figure 2.7 and pressure profile is shown in figure 2.8. The application of the principle of superposition in time to the analysis is quite simple. The drawdown at a rate, q, prior to the build-up, is assumed to continue for all time, $t_p+ \Delta t/\Delta t$, but at the time of shut-in, t_p, a drawdown at a rate, -q, is initiated. The net effect of a negative rate, or injection, is to simulate a flow rate of zero, which is the shut-in condition. Hence any shut-in time, Δt, the pressure behavior at the well will be the sum of two effects, that due to a flow rate q for a time ($t_p+ \Delta t/\Delta t$), and that due to a flow rate -q for a time Δt. This treatment is identical to that for a two-rate drawdown test with the second rate, q_2, taken equal to zero. This gives us a means to generate the pressure response during a buildup test, using the simple constant rate solutions generated for drawdown tests (as in Eq. 2.15).

$$p_D(t_D) = p_D(t_{p^D} + \Delta t_D) - p_D(\Delta t_D) \quad \text{.....(2.15)}$$

This is illustrated in Fig. 2.7, and is true regardless of the reservoir model used.

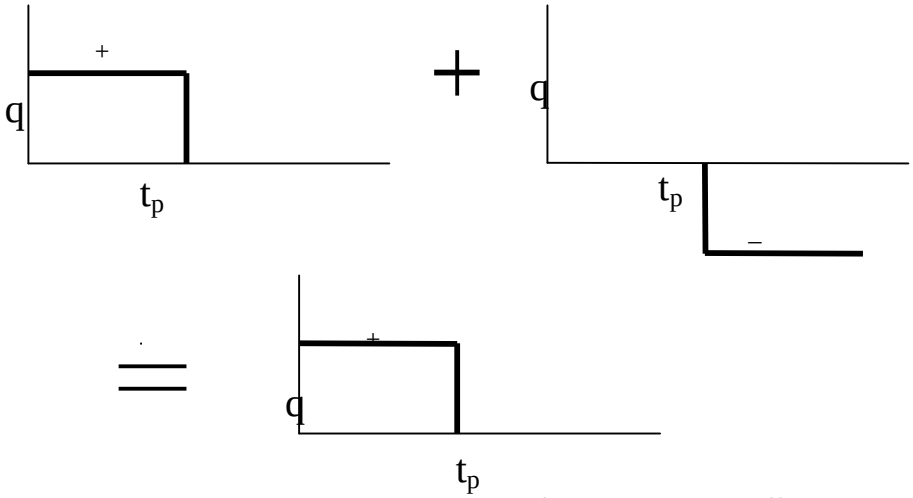

Figure 2.7: Build-up treated as the result of two superposed effects

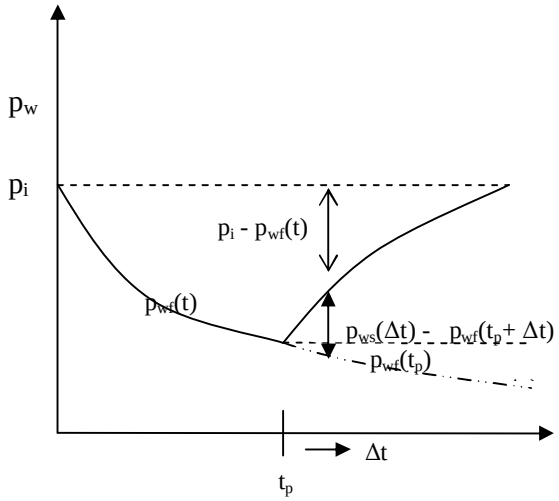

Figure 2.8: Pressure profile for superposed effects

While discussing this point, we can observe that this time superposition leads to a particularly simple result during infinite acting radial flow. During this flow regime:

$$p_{ws} = p_i - \frac{141.2_{qBm}}{kh}\left[\frac{1}{2}\left(In\frac{k(t_p+\Delta t)}{fmc_t r_w^2} - In\frac{k\Delta t}{fmc_t r_w^2}\right)\right] \quad \text{.....(2.16)}$$

$$or,\ p_{ws} = p_i - \frac{162.6_{qBm}}{kh}\log\frac{(t_p+\Delta t)}{\Delta t} \quad \text{.....(2.17)}$$

Thus a plot of pressure against the logarithm of $(t_p + \Delta t)/\Delta t$ will show a straight line of slope:

$$m = \frac{162.6qBm}{kh}$$

Such a plot is known as a Horner plot, and we refer to $(t_p + \Delta t)/\Delta t$ as the Horner time (Fig.2.9). Due to the definition of Horner time, it should be noted that actual time increases to the left in Fig. 2.9. As the shut-in time Δt tends to infinity, the Horner time $(t_p + \Delta t)/\Delta t$ tends to 1.

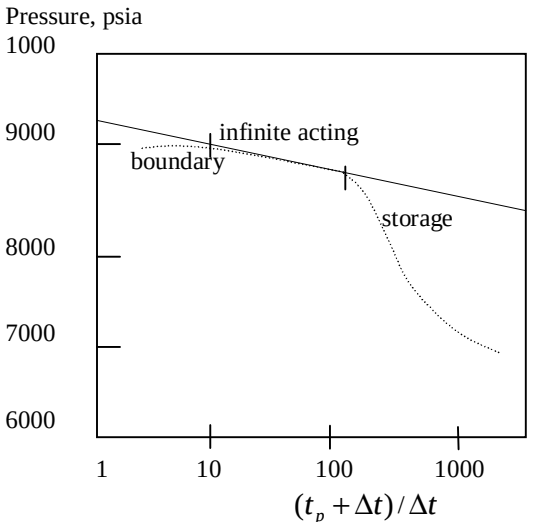

Figure 2.9: Horner plot

The Horner plot may also be used to extimate the skin factor. Since the skin factor is a dimensionless perssure drop, the skin effect only influences the flowing period of the test. Thus it is necessary to include the data point repersenting the last flowing pressure—this point is

$$p_{ws}(t_p + \Delta t) - p_{wf}(t_p) = \frac{1}{2}\frac{141.2qBm}{kh}\left[\ln\frac{t_p \Delta t}{t_p + \Delta t} + 0.80907 + \ln\frac{0.000264k}{fmc_t r_w^2}\right] + s$$

If we substitute a value of Δt +1 hour, then we can obtain an estimate of the skin factor:

$$s = 1.151\left[\frac{p_{1hr} - p_{wf}}{m} - \log\frac{kt_p}{(t_p + 1)fmc_t r_w^2} + 3.2274\right]$$

As with drawdown tests, it is important to note that the value of p1hr needs to be taken from the Horner straight line, or the extrapolation of it. This is due to the assumption of infinite-acting radial flow—the flow regime at the regime at the arbitrary time of 1 hour may not be infinite-acting, and therefore the actual pressure data point at this time is not the correct one to use.

Initial Pressure (P_i)

The initial pressure is the average reservoir pressure before the start of a test. For a new well (a well which has not been put on production), the initial pressure equals the virgin or original reservoir pressure and corresponds to the drill stem test (DST) pressure. For a well that has been on production for a long time the initial pressure may or may not be equal to the original reservoir pressure. The following example illustrates this concept.

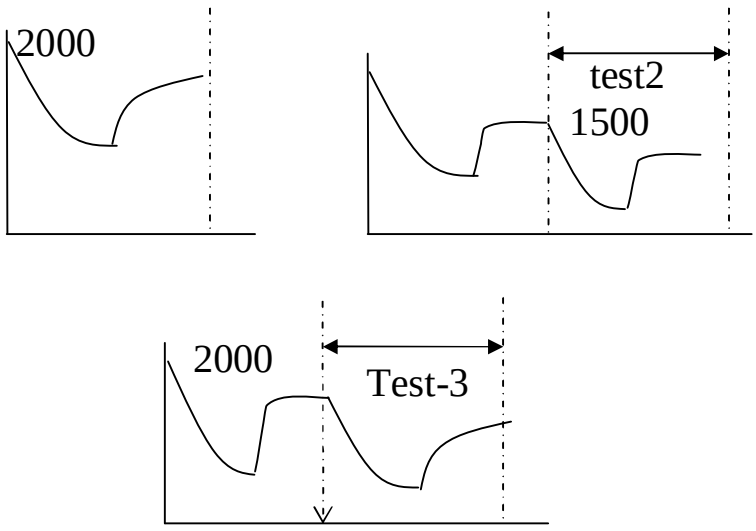

Figure 2.10: Illustration of Initial Pressure (Pi)

In the above diagram if Test 1 is being analyzed, the initial pressure is 2000. If Test 2 is being analyzed, the initial pressure is 1500, because the reservoir pressure is fully built up before this test and the reservoir has forgotten its history prior to Test 2. Thus it behaves like a new well with an initial pressure 1500. If Test 3 is being analyzed (which is a combination of Test 2 and some production prior to Test 2), then the initial pressure is 2000, because it must reflect the reservoir pressure before the production that is being analyzed during the test.

Log-log Type Curves

It should be noted semilog analysis uses only part of the data (the semilog straight line) to estimate the unknown reservoir parameters. Since the early part of the reservoir response is usually overshadowed by wellbore storage effects, we need to wait until the semilog straight line is visible before a semilog analysis can be performed. Since we know that there is usually about 1½ log cycles of data between the end of wellbore storage and the start of the semilog straight line, we might wonder if there is some way to use this transitional data as well in our analysis. One alternative to semilog analysis that uses the transitional data is log-log type curve analysis. Log-log type curve analysis makes use of the dimensionless variables described in "2.2 Dimensionless Variables" on page 7. Since, by definition, dimensionless pressure and time are linear functions of actual pressure and time (recall Eqs. 2.3 and 2.4), then the logarithm of actual pressure drop will differ from the logarithm of dimensionless pressure drop by a constant amount.

$$\log \Delta p = \log p_D - \log \frac{kh}{141.2qBm}$$

similarly

$$\log t = \log t_D - \log \frac{0.000264k}{fmc_t r_w^2}$$

Hence a graph of log p versus log t will have an identical shape to a graph of log p_D versus log t_D, although curve will be shifted by log kh/141.2aB vertically (in prcssure) and log (0.000264 k/ $fmc_t r_w^2$) horizontally (in time). Matching the two curves will give us estimates of hk from kh/141.1 qBm (assuming q, B and m are known) and (from (0.000264k/ $fmc_t r_w^2$, assuming and are known). This process provides a useful method of estimating two very important reservoir parameters, the transmissivity or ability to flow, and the storability or quantity of fluid contained. Type curves can be used to estimate other parameter—this will be illustrated in examples.

Modern Analysis Technique

Modern analysis has been greatly enhanced by the use of the derivative plot introduced by Bourdet, Whittle, Douglas and Pirard (1983), also discussed in Bourdet, Ayoub and Piraed (1989). The derivative plot provides a simultaneous presentation of log p vs. log t and log tdp/dt vs. log t. The advantage of the derivative plot is that it is able to display in a single graph many separate characteristics that would otherwise require different plots.

Other Flow Regimes

Fluid flows in the reservoir in different ways at different times. This is often a function of the shape and size of the reservoir. The basic flow regimes, shown in table 2.1, are categorized in terms of which time region they occur and what kind of wellbore (vertical or horizontal) was used to drill into the formation. Different types of flow regimes are briefly introduced below.

Wellbore Storage

Wellbore Storage is caused when the flow rate at the wellhead is different than the flow rate at sandface. It is usually caused by wellbore unloading, Afterflow Analysis, or changing fluid levels. Data affected by wellbore storage effects contain little or no information about the reservoir. The purpose of analyzing afterflow data is to determine the wellbore storage constant Cs, and to determine when afterflow ends and reservoir dominated data begins

The constant rate solution for analyzing afterflow data, for gas, is:

$$\Delta y = 2348 \frac{qTt_a}{m_{ti} C_s}$$

Wellbore Storage Constant

The slope of the p versus Δta line is used to calculate the wellbore storage constant:

$$C_s = 2348 \frac{qTt_a}{m_{ti} slop}$$

Bilinear Fracture Flow

Bilinear fracture flow, shown in figure 2.10, occurs in hydraulically fractured wells when the conductivity of the fracture is finite. In this flow regime, two types of linear flow occur: one from the matrix to the fracture and one from the fracture to the wellbore. This is usually evident in long fractures (which are hard to prop open effectively) or in natural fractures (which contain fracture fill minerals).

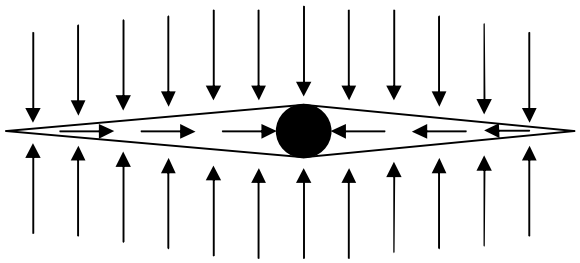

Figure.2.11 Bilinear fracture flow for a vertical well

Linear Fracture Flow

Linear fracture, shown in figure 2.10, flow occurs in hydraulically fractured wells when the conductivity of the fracture is infinite. In this situation the permeability of the fracture is so high that the pressure throughout the fracture is constant

.

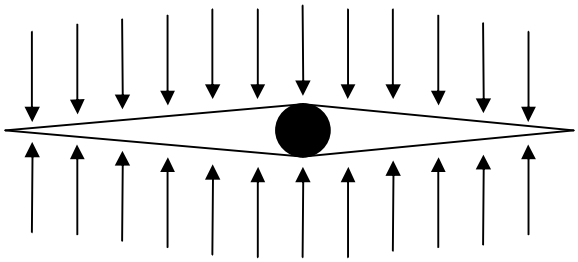

Figure.2.12 Linear fracture flow for a vertical well.

Linear Channel Flow

Linear channel flow only occurs in long, narrow reservoirs. Initially the radius of investigation hasn't reached the reservoir boundaries and radial flow is observed. After the two parallel boundaries have been reached, a period of linear channel flow can be observed.

Well Located Near a Single no Flow Boundary

A no flow boundary can be a physical entity, such as a sealing fault, or can occur when two producing (or two injecting) wells are adjacent to one another. Mathematically, a situation

in which a well is next to a sealing fault can be modeled by removing the fault and placing an image well with a flow rate equivalent to the producing well.

Transition between Middle and Late Time Regions

The transition period occurs between the time the radius of investigation reaches the closest boundary and the time it reaches the furthest boundary.

Late Time

The Late Time region begins when the radius of investigation has reached all of the boundaries..During this time period, stabilized flow has been reached.

Table 2.1: Different types of flow regimes

	Early Time	**Middle Time**	**Transition**	**Late Time**
Vertical Wells	Wellbore Storage Linear - Fracture Bilinear- Fracture Spherical	Radial	Well close to no-flow boundary Linear Channel	Pseudo-Steady State Steady State
Horizontal Wells	WellboreStorage Vertical Radial Linear Elliptica	Radial	Linear Channel	Pseudo-Steady State Steady State

CHAPTER 3

Different Types of Well Based on Reservoir Modeling

A well produces what a reservoir permits through it. There are different types of well, based on the production of the well and physical structure of the reservoir—single layer, multi layer, bounded by sealing rock etc. In this chapter wells are classified according to the fluid, sometimes shows special characteristics due to change in pressure, flows through the reservoir and the size and shape of the reservoir.

3.1 Testing Gas Condensate Wells

Reservoirs bearing gas-condensates are becoming more common as developments are encountering greater depths, higher pressures, and higher temperatures. Accuracy in engineering computations for gas-condensate systems (e.g., well testing, estimating reserves, sizing surface facilities, and predicting productivity trends) depends upon a basic understanding of phase and flow behavior relationships. When we compare dry- gas reservoirs with gas-condensate reservoirs, there are many special factors that affect the performance of gas-condensate reservoir during the exploitation process.

At the time of discovery, a typical gas-condensate reservoir pressure might be above or close to the critical pressure. At this time there exists only single-phase gas. If the initial reservoir condition were represented by point A_1 on the pressure-temperature phase diagram of Figure 3.1, then the isothermal pressure decline during reservoir depletion would follow the line A_1-A_4. Because the initial reservoir pressure is above the upper dew-point pressure, the hydrocarbon system exists as a single phase (i.e., vapor phase) and remains so during the isothermal decline path A_1-A_2. As the reservoir pressure drops below point A_2, the dew-point will be passed and a liquid phase will develop in the reservoir. Liquid dropout will continue to increase and reaches a maximum dropout at point A3. However, at point A_4, the dew-point curve must be crossed again. This means that all the liquid, which formed, must vaporize because the system is essentially all vapors at the lower dewpoint. The productivity loss associated with condensate buildup can be substantial. Afidick et al. (1994) and Barnum et al. (1995) have accounted for several instances in which well productivities have been reported to decline by a factor of two to four as a result of condensate accumulation.

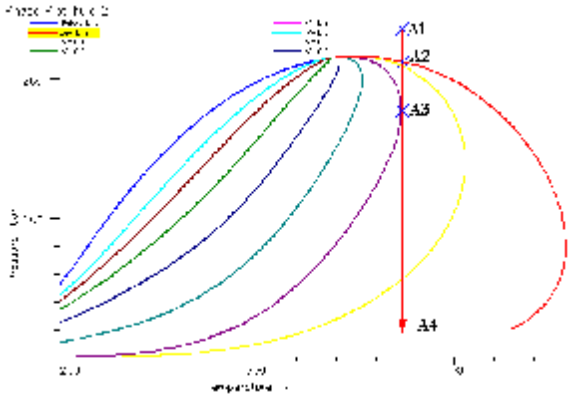

Figure 3.1: Phase envelope diagram of gas-condensate mixture

The liquid dropout first occurs near the wellbore and propagates radially away from the well (assuming the well at the center of a radial reservoir) along with the pressure drop. Fevang (1995) and Ali et al. (1997) showed that, when reservoir pressure around a well drops below the dew-point pressure, retrograde condensation occurs and three regions are created with different liquid saturations. Away from the well, an outer region has the initial liquid saturation; next, there is an intermediate region with a rapid increase in liquid saturation and a corresponding decrease in gas relative permeability.

Gas condensate reservoirs exhibit complex behavior at pressures below the dew point due to condensate drop out in the reservoir, especially in the vicinity of the well. Consequently, zones of different mobility and composition exist at varying distances from the well. Moreover, close to the well, we will have two-phase flow (gas and condensate) while further away from the reservoir, the fluid exists only as a gas, if the pressure is above the dew point pressure. The layer closest to the well has one set of fluid properties and the region farther away has different fluid properties (See Figure 3.2)

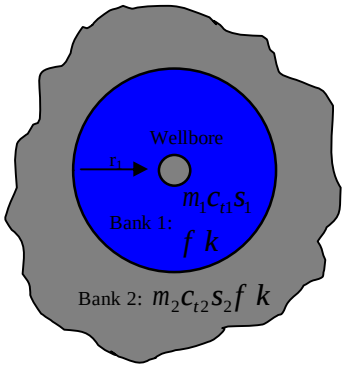

Figure 3.2.Formation of a condensate ring around the wellbore.

Due to the condensate formation, the ability of the gas to flow is hindered. As a result of the formation of a condensate bank around the wellbore, we will often see pressure responses from a condensate ring around the well, from a transition bank farther away and if the test is long enough, from the single phase reservoir gas even farther away. This complicates analysis of well tests since the skin associated with the zone closer to the well is due to completion skin effects in addition to the condensate dropout. However, gas condensate wells can and often exhibit even more complex behavior in the pressure responses. Depending on the flow rates, there might be a zone in the immediate vicinity of the well where capillary number effects dominate and we might have a zone of increased permeability to gas. Farther away, in a transition zone, the gas might be dropping condensate and flow velocities may not be high enough for capillary number effects to dominate. In these zones, we might have lower permeability to gas. Even farther away, where the reservoir pressure is above the dew point, we will have single phase gas and the permeability obtained will be indicative of reservoir permeability.

3.2 Testing Multi-Layer Formations in Bounded Reservoirs

Multilayer formations consist of two or more layers. Each layer has different properties and the pressure transients from all the layers contribute to an integrated response in the pressure transient test. A schematic of the 2 layer formation type selected for this interpretation is shown in Figure 3.3.

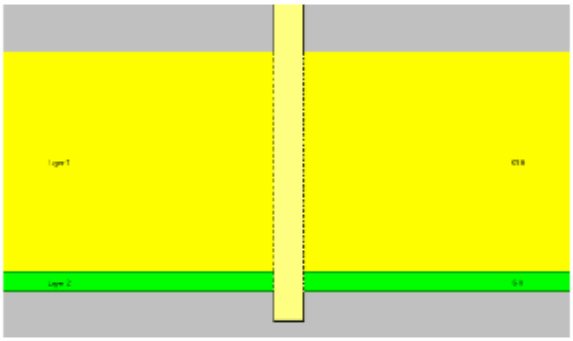

Figure 3.2: schematic of the 2 layer formation.

In the absence of boundaries, the 2 layer formation would behave like a single layer formation of average properties from both the layers. However, if the pressure transients during the test reach a boundary, then the analysis is more complicated. Particularly when the boundary is a closed boundary, a typical response is a positive unit slope line on the late-time pressure derivative response.

3.3 Testing Gas Wells in Bounded Reservoirs

During a pressure build-up, the derivative response first shows the effects of wellbore storage. This is followed by an infinite acting radial flow regime, which may or may not be masked by the wellbore storage effect. If the pressure transient reaches a boundary, either with a constant pressure or a closed boundary, the build-up pressure derivative drops sharply. Consequently, it is not possible with a build-up analysis to determine if the reservoir has a closed boundary or a constant pressure boundary (eg. Aquifer). With drawdown tests, it is easier to distinguish between a closed boundary and a constant pressure boundary. However, with drawdown tests the analysis is complicated due to noise in the measured rates because it is difficult to maintain a constant rate effectively over the duration of the test. With deconvolution of the response, it is possible to interpret drawdown tests accurately, but this requires downhole flow gauges which will record the downhole flow rates. A downhole shut-in is also recommended to minimize the effects of wellbore storage.

CHAPTER 4

Diagnosis of Different Producing Wells of SGFL

In this chapter, data collected from different producing wells of different field of SGFL are analyzed. To analyze and to interpret collected data, Special type of computer software, F.A.S.T. WellTest, is used. At first, data collected from 3 (three) wells of Kailashtilla Gas Field are analyzed to determine different formation and well characteristics. Then, 2 (two) wells of Biany Bazar Gas Field and finally 3 (three) wells of Rashidpur Gas Field are analyzed. The findings of each gas field are summarized in a separate table at the end of the particular section.

4.1 Kailashtilla Gas Field

The lithology of the Kailashtilla gas field is complex and is comprised of quartz, feldspars, micas and heavy minerals. The Kailashtilla anticline is 17 km long and 5 km wide on an average. Early estimates of the in-place gas reserves of Kailashtilla Field were made by assuming a uniform distribution of thickness of the Upper Gas Sands (179 ft), Middle Gas Sands (69ft) and Lower Gas Sands (166 ft), as encountered in Well KTL#1, over the entire closure as mapped then. Subsequent wells KTL#2 and KTL#3 have indicated an entirely different pattern of thickness distribution of each of the three sands. The Upper Gas Sand thickness to the north to 322 ft in well KTL#3; the Middle Gas Sand thickness to the north to 175 ft in well KTL#3; whereas the Lower Gas Sand thins abruptly to 45 ft in well KTL#2 and 30 ft in well KTL#3 (IKM, 1989).

The study of the Kailashtilla Gas Field, from core data analysis of KTL#1, focuses on reserves in three distinct horizons, being the regions defined as following tables.

Table 4.1: Different Producing Sands and Geo-physical Properties of Kailashtilla Gas Field

Horizon	Interval		Thickness, h, ft	Average Permeability, k, md (From Core Data Analysis)	Average Porosity, ø, Fraction
	ft KB	ft ss			
Upper Gas Sand	7483 - 7662	7422 - 7601	179	424.3	0.18
Middle Gas Sand	9665 - 9734	9604 -9673	69	88.4	0.19
Lower Gas Sand	9808 - 9990	9747 - 9913	166	189.6	0.21

Table 4.2: Different Producing Well and Their Producing Sands of Kailashtilla Gas Field

Well	Producing Zone
KTL#1	Middle Gas Sand
KTL#2	Upper Gas Sand
KTL#4	Middle Gas Sand

There are six producing gas wells in Kailashtilla Gas Field. Well no KTL#1, KTL#2 and KTL#4 were available for well testing. Gas produced from Well no KTL#2, KTL#3 and KTL#4 is processed by Molecular Sieve Turbo Expander (MSTE) plant, and gas produced from well no KTL#1 is processed by a separate Silica gel Plant in different location. Detail well test diagnosis scenario is presented for Well no KTL#1, KTL#2 and KTL#4 in the following subsection.

4.1a KTL#1

The intervals tested are three perforation intervals in the Middle Gas Sand from a depth of 9652 ft to 9655 ft, 9658 ft to 9664 ft and 9668 ft to 9722 ft for a total perforation length of 65 ft. Detailed fluid report has not available, but the fluid is reported to be a gas condensate. This is reasonable because the observed condensate gas ratio at stock tank conditions during the test was 8 STB/ Mscf. For these high values of condensate gas ratio, it may be treated as a wet gas at reservoir conditions. This implies that the gas is not expected to drop condensate in the vicinity of the wellbore during production and there will be no production impairment due to condensate dropout (Almansoori). PVT properties of the reservoir fluid should be determined to find out the nature of the reservoir whether it is dry gas reservoir or wet gas reservoir or retrograde reservoir. Production testing for this well was carried out at the Kailastilla station process plant separator. Before buildup test, the well is flown for 3 different flow rates, (11.0782 MMcfd, 3453 psia) for 8.1 hours, (16.22 MMcfd, 3465 psia) for 14.3 hours and (18.8 MMcfd, 3440 psia) for 5.6 hours.

Pressure Transient Analysis Plots

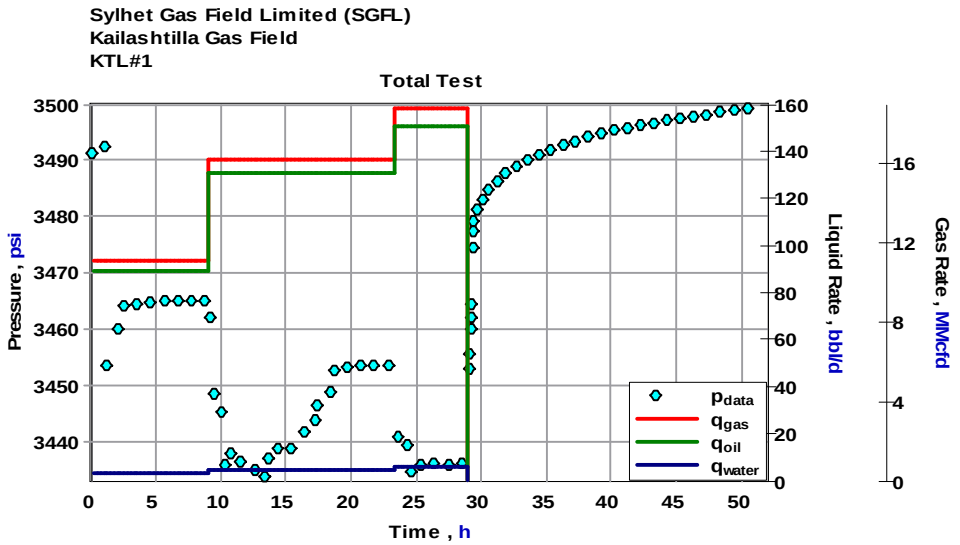

Figure 4.1: Total test data plot of KTL # 1

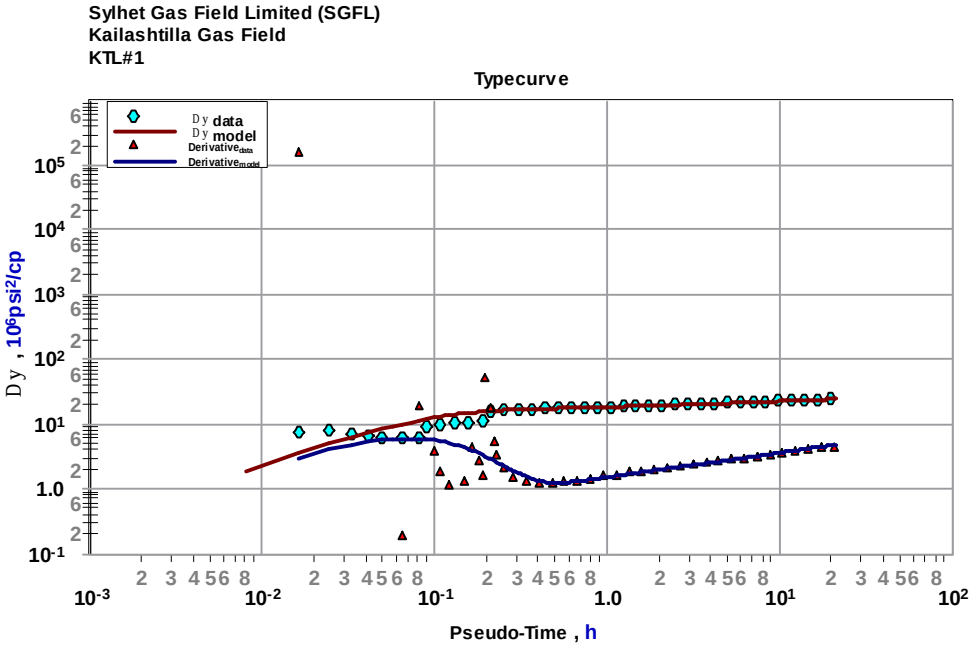

Figure 4.3: Type curve plot of KTL # 1

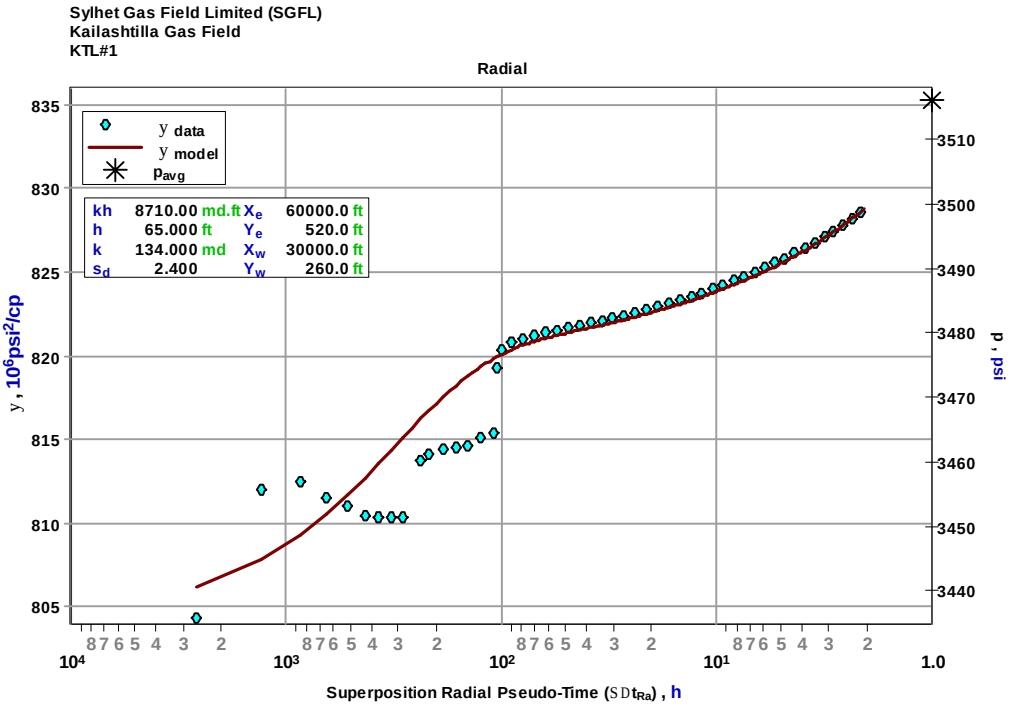

Figure 4.3: Radial analysis and pressure matching of KTL # 1

Figure 4.1 shows the variation of flow rates of gas (MMcfd), condensate (bbl/d) and water (bbl/d) with pressure (psia) and time (h). Figure 4.2 shows the type curve matching where variation of difference of pseudo pressure ($\Delta y 10^6 psi^2/cp$) and derivative of pseudo pressure of actual field data with respect to pseudo time (h) are matched with synthetic model data, generated from computer software. Figure 4.3 shows the variation of pseudo pressure ($y 10^6 psi^2/cp$) with respect to superposition radial pseudo time (h) and, pseudo pressure of actual field data are matched with synthetic model data.

Results

Results of analysis are shown in table 4.3 along with the results of Almansoori and IKM.

Table 4.3: Reservoir/Well Parameters of KTL#1 by Different Analysts (Author of this Report, Al-monsure and IKM)

Reservoir/Well Parameters	**Author of This Report**	**Almansoori**	**IKM**
Model Characteristics	Vertical	Standard with Changing Wellb Storage	IKM did not carry out any Pressure-transient analysis for middle Gas Sands.
Reservoir Parameters			
Total Permeability-thickness Product, kh (md. ft)	10855	9550	
Average Permeability, K (md)	134	147	
Initial Reservoir Pressure, Pi (Psia)	3516.2	3515	
Well and Wellbore Parameters			
WellboreStorage Coefficient, C (bbl/psi)	2.6e-05	0.154	
Skin, S	2.4	3	

From Table 4.3, it is clear that all Reservoir Parameters and Well and Wellbore Parameters except WellboreStorage Coefficient, find out by two different analysts, Author of This Report and Almansoori, are almost similar. However, from core data analysis, Average Permeability of the Middle Gas Sand, from where KTL#1 is producing, is 88.4 md (Table 4.1). Difference of WellboreStorage Coefficient between the results of two analysts may be occurred due to different model characteristics.

4.1b KTL#2

The interval tested is the Upper Gas Sand from a depth of 7390 ft to 7430 ft. Detailed fluid report has not available, but the fluid is reported to be a gas condensate. This is reasonable because the observed condensate gas ratio at stock tank conditions range from 8.2 STB/MMscf to approximately 8.0 STB/MMscf. Although the gas is reported to be a gas condensate, for these high values of condensate gas ratio, it may be treated as a wet gas at reservoir conditions. This implies that the gas is not expected to drop condensate in the vicinity of the wellbore during production and there will be no production impairment due to condensate dropout (Almansoori). Production testing for this well was not carried out because the process plant separator gas flow meter was not working at the time of the test. Gas flow rates were not reported correctly i.e. some part of gas flows from other wells (KTL#1, KTL#3 and KTL#4) is consider as flows from KTL#2, and the analysis is performed on the build-up portion of the test. It is recommended that another production test be run to infer formation characteristics. There is some minor evidence of a rate dependant skin, but as mentioned earlier, these values may be erroneous due to no measurements available for the actual gas flow.

Pressure Transient Analysis Plots

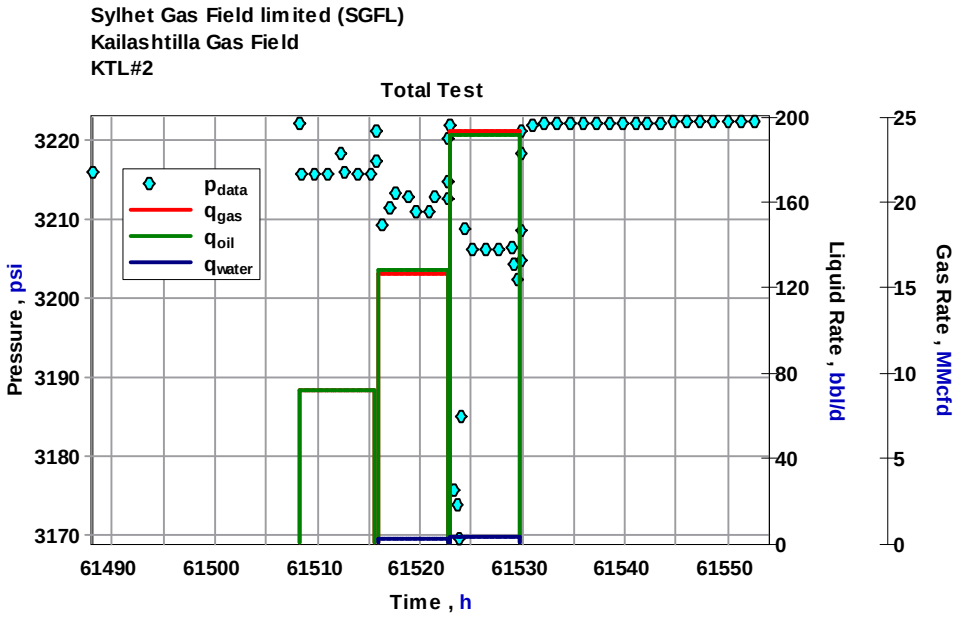

Figure 4.4: Total test data plot of KTL # 2

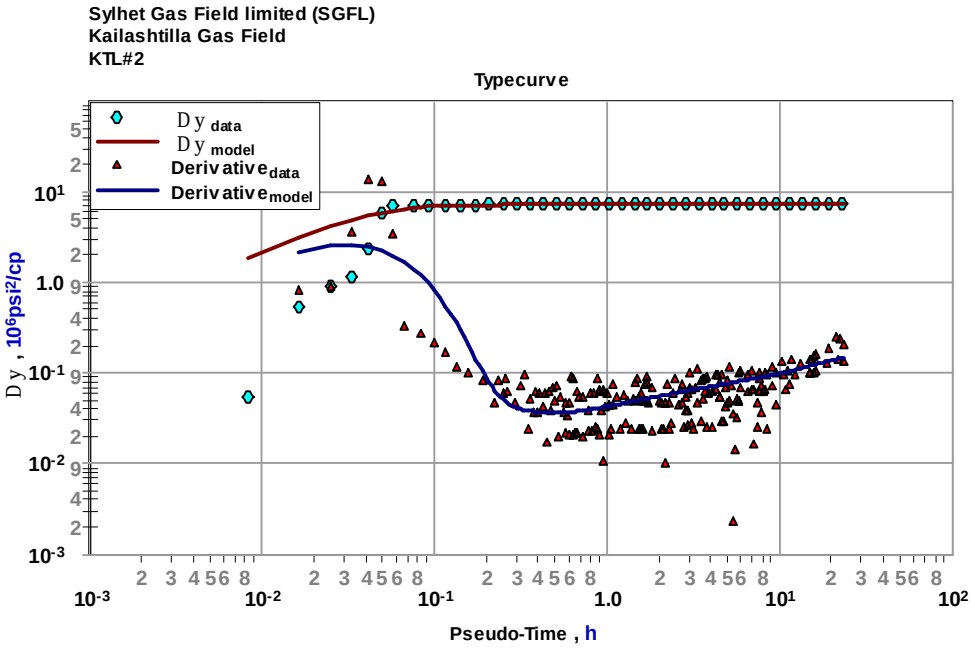

Figure 4.5: Type curve plot of KTL # 2

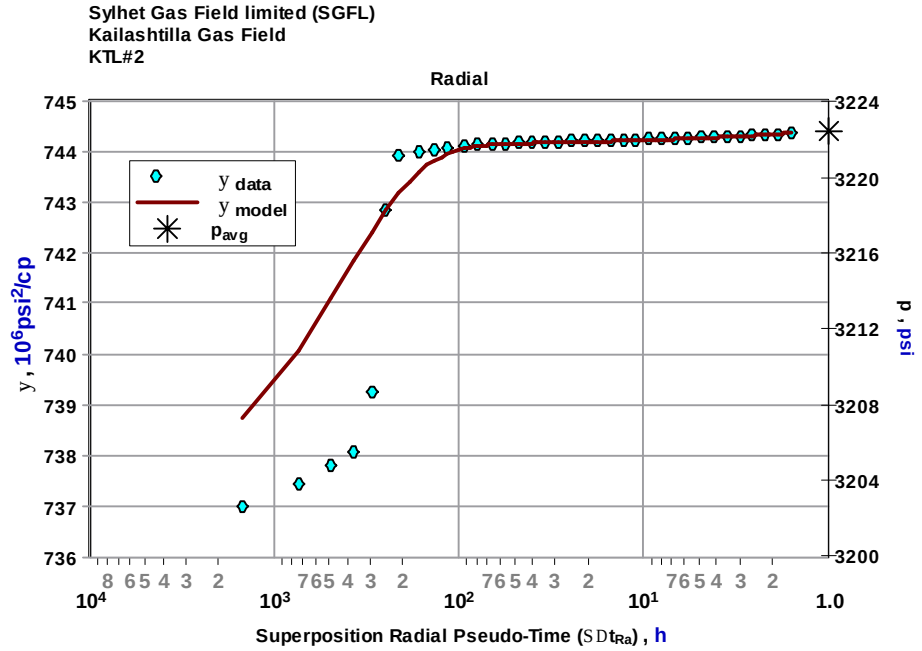

Figure 4.6: Radial analysis and pressure matching of KTL # 2

Figure 4.4 shows the variation of flow rates of gas (MMcfd), condensate (bbl/d) and water (bbl/d) with pressure (psia) and time (h). Figure 4.5 shows the type curve where variation

of difference of pseudo pressure ($\Delta y 10^6 psi^2/cp$) and derivative of pseudo pressure of actual field data with respect to pseudo time (h). Here, derivative of pseudo pressure of actual field data are very scattered, and inaccuracy in measurement of gas flow rates is the possible cause of scatterings. Figure 4.6 shows the variation of pseudo pressure ($y 10^6 psi^2/cp$) with respect to superposition radial pseudo time (h) and, pseudo pressure of actual field data are matched with synthetic model data.

Results

Results of analysis are shown in table 4.4 along with the results of Almansoori and IKM.

Table 4.4: Reservoir/Well Parameters of KTL#2 by Different Analysts (Author of this Report, Al-monsure and IKM)

Reservoir/Well Parameters	**Author of This Report**	**Almansoori**	**IKM**
Model Characteristics	Verticalwell	Standard with Changing Wellbore Storage	IKM did not carry out any Pressure-transient analysis for KTL#2.
Reservoir Parameters			
Total Permeability-thickness Product, kh (md. ft)	2.2e+05	1.97e+05	
Average Permeability, K (md)	5575	4700	
Initial Reservoir Pressure, Pi (Psia)	3223.3	3221	
Well and Wellbore Parameters			
WellboreStorage Coefficient, C (bbl/psi)	24.83	1.5	
Skin, S	4.1	25	

From Table 4.4, it is clear that all Reservoir Parameters and Well and Wellbore Parameters except Initial Reservoir Pressure, find out by two different analysts, Author of This Report and Almansoori, show dissimilarity. However, from core data analysis, Average Permeability of the Upper Gas Sand, from where KTL#2 is producing, is 424.3 md (Table 4.1). During the pressure transient data collection of this test, gas flow rates were not reported correctly as gas flow meter did not work properly. Consequently, all the data and results reported in this section may not be very accurate or representative of the formation characteristics.

4.1c KTL#4

The interval tested is the Middle Gas Sand from a depth of 9610 ft to 9673 ft and 9696 ft to 9702 ft. Detailed fluid report has not available, but the fluid is reported to be a gas condensate. This is reasonable because the observed gas condensate ratio at stock tank conditions range from 7.88 STB/MMscf to approximately 8.1 STB/MMscf. Although the gas is reported to be a gas condensate, for these high values of gas condensate ratio, it may be treated as a wet gas at reservoir conditions. This implies that the gas is not expected to drop condensate in the vicinity of the wellbore during production and there will be no production impairment due to condensate dropout (Almansoori). The pressure transients show that this reservoir could be bounded, because a positive approximately unit slope line on the late-time pressure derivative response is observed. Test duration must be longer in future test to extend the pressure derivative response, which will help to justify the formation nature.

Pressure Transient Analysis Plots

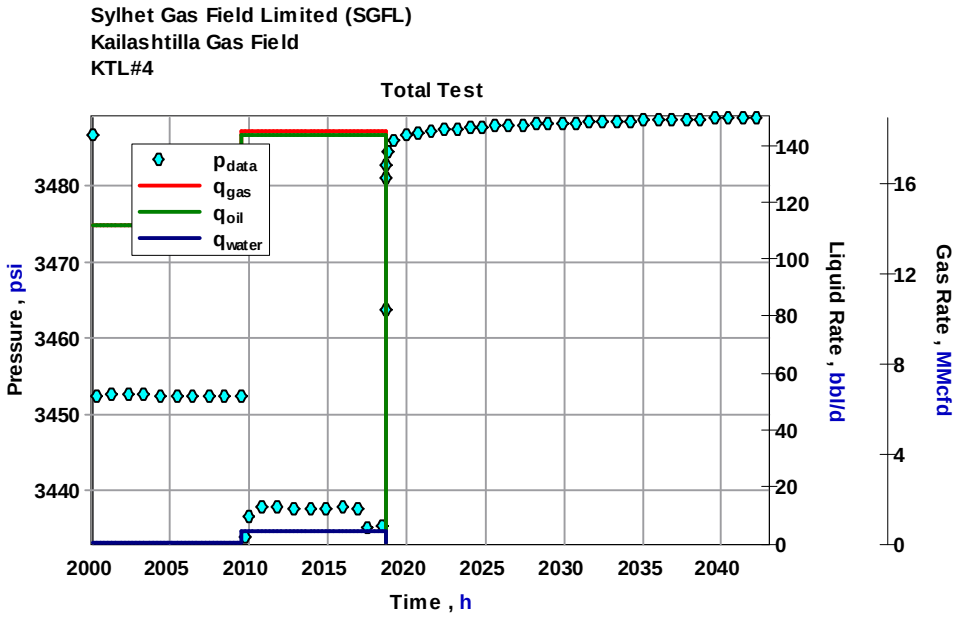

Figure 4.7: Total test data plot of KTL # 4

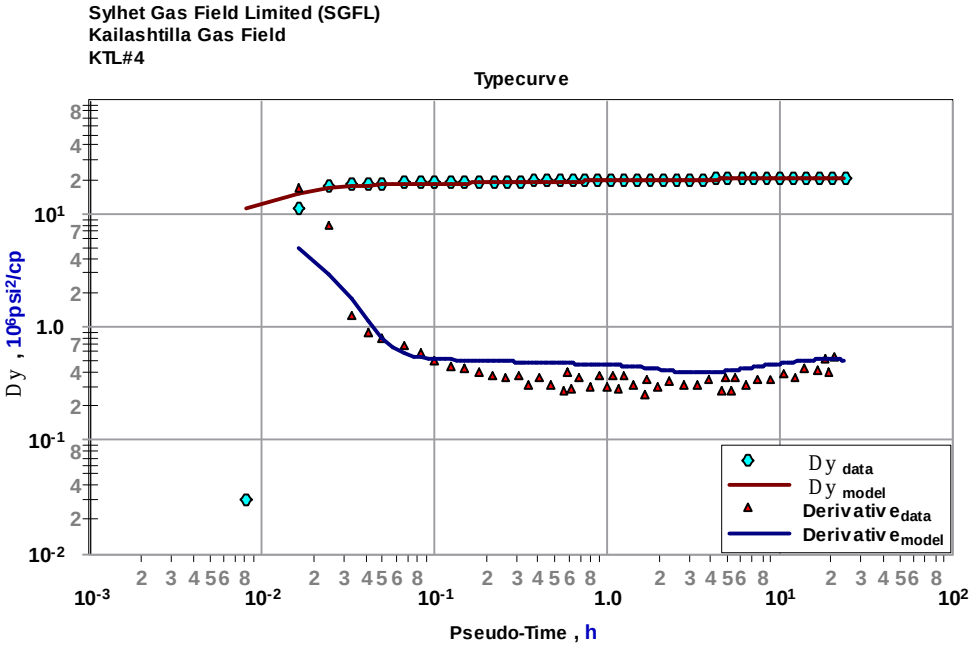

Figure 4.8: Type curve plot of KTL # 4

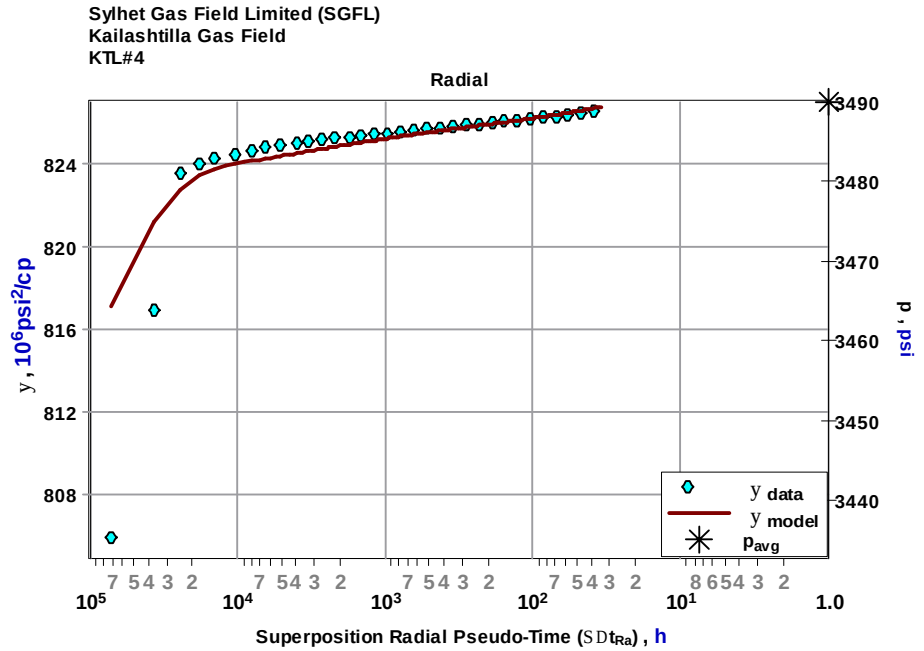

Figure 4.9.Radial analysis and pressure matching of KTL # 4

Figure 4.7 shows the variation of flow rates of gas (MMcfd), condensate (bbl/d) and water (bbl/d) with pressure (psia) and time (h). Figure 4.8 shows the type curve matching where variation of difference of pseudo pressure ($\Delta y 10^6 psi^2/cp$) and derivative of pseudo pressure of actual field data with respect to pseudo time (h) are matched with synthetic

model data, generated from computer software. Here, late time response of derivative of pseudo pressure of actual field data shows upward trend, which indicates the near boundary effect. Figure 4.9 shows the variation of pseudo pressure ($y10^6$psi^2/cp) with respect to superposition radial pseudo time (h) and, pseudo pressure of actual field data are matched with synthetic model data.

Results

Results of analysis are shown in table 4.5 along with the results of Almansoori and IKM.

Table 4.5: Reservoir/Well Parameters of (KTL#4) by Different Analysts (Author of this Report, Al-monsure and IKM)

Reservoir/Well Parameters	**Author of This Report**	**Almansoori**	**IKM**
Model Characteristics	Vertical well	Standard with Constant Wellbore Storage	IKM did not carry out any Pressure-transient analysis for middle Gas Sands.
Reservoir Parameters			
Total Permeability-thickness Product, kh (md. ft)	16422	23600	
Average Permeability, K (md)	238	342	
Initial Reservoir Pressure, Pi (Psia)	3489.9	3490.6	
Well and Wellbore Parameters			
WellboreStorage Coefficient, C (bbl/psi), (bbl/psi)	0.24	0.179	
Skin, S	9.8	20.6	

From Table 4.5, it is clear that Initial Reservoir Pressure and WellboreStorage Coefficient, C (bbl/psi) show similarity but not other parameters. However, from core data analysis, Average Permeability of the Middle Gas Sand, producing zone of KTL#4, is 88.4 md (Table 4.1). Two main parameters, Average Permeability and Skin, show huge dissimilarity. This is a composite reservoir, paying from two different zone, and pseudo pressure derivative curve in figure 4.8 indicates the bounded nature, a positive approximately unit slope line on the late-time pressure derivative response, of the reservoir. Hence, Pressure-transient data should have analyzed by using different model and decision should be taken with matching geological data.

4.2 Biany Bazar Gas Field

Biany Bazar Gas Field, situated in the north-east corner of Bangladesh, is one of the most resourceful gas fields of Sylhet Gas Field. There are two producing gas wells, BB#1 and BB#2. Gas produced from Well no BB#1 and BB#2 is processed by Silica gel Plant in a location about three Km away from the well.

The lithology in the biany bazar gas reservoir varies and is very complex. The rock is comprised of quartz, feldspars, micas and heavy minerals.

The Biany Bazar field comprises of two layers, upper sand, between 10,599 and 10,755 ft kB, and lower sand, between11,324 to11,370 ft kB of the well BB#1. As per a previous reservoir engineering report, the proven gas in place in 1999 was 187.0 Bcf and 56.10 Bcf respectively for the upper gas sand and the lower gas sand. Total production from May 1999 to October 2007 was 27.78 Bcf from the lower gas sand and 21.08 Bcf from the upper gas sand. 2 wells were completed in this field, BB#1 was completed in the lower gas sand and BB#2 was completed in the upper gas sand.

Here, well test data, available for well no BB#1 and BB#2, is analyzed to determine the formation characteristic (permeability) and completion characteristic (skin) of the well, any reservoir barriers to flow in the vicinity of the well, current reservoir pressure, temperature, liquid holdup etc

Different Producing Sands, Producing Wells and Geo-physical Properties of Biany Bazar Gas Field are shown in following tables.

Table 4.6: Different Producing Sands and Geo-physical Properties of Biany Bazar Gas Field

Horizon	Interval		Thickness, h, ft	Average Permeability, k, md (From Core Data Analysis)	Average Porosity, ø, Fraction
	ft KB	ft ss			
Upper Gas Sands	10599-10755	10787-10804	121	332.4	0.22
Lower Gas Sand	11324-11370	11523-11549	42	189.6	0.21

Table 4.7: Different Producing Well and Their Producing Sands of Biany Bazar Gas Field

Well	Producing Zone
BB#1	Lower Gas Sand
BB#2	Upper Gas Sand

4.2a BB#1

BB#1 was completed in the lower gas sand. Total production from May 1999 to October 2007 was 27.78 Bcf from the lower gas sand. Initial total production was 30 MMscf/day from both the wells; however, due to increasing water production the daily average production has dropped to 15 MMscf/day. The general tendency has been an increase in water produced and this has been difficult to control. Probable causes could be water coning from an underlying aquifer in both the wells, which might need to be controlled or mitigated (Almansoori). Detailed fluid report has not available, but the fluid is reported to be a gas condensate. This is reasonable because the observed condensate gas ratio at stock tank conditions range from 13 to 20 STB/MMscf. Consequently, it is also expected that a condensate bank may have formed in the vicinity of the wells due to previous production and subsequent well draw down during production testing. It is expected that this will impact the well test analyses. Any information about the dew point pressure or whether this has been reached in the reservoir is not available.

Pressure Transient Analysis Plots

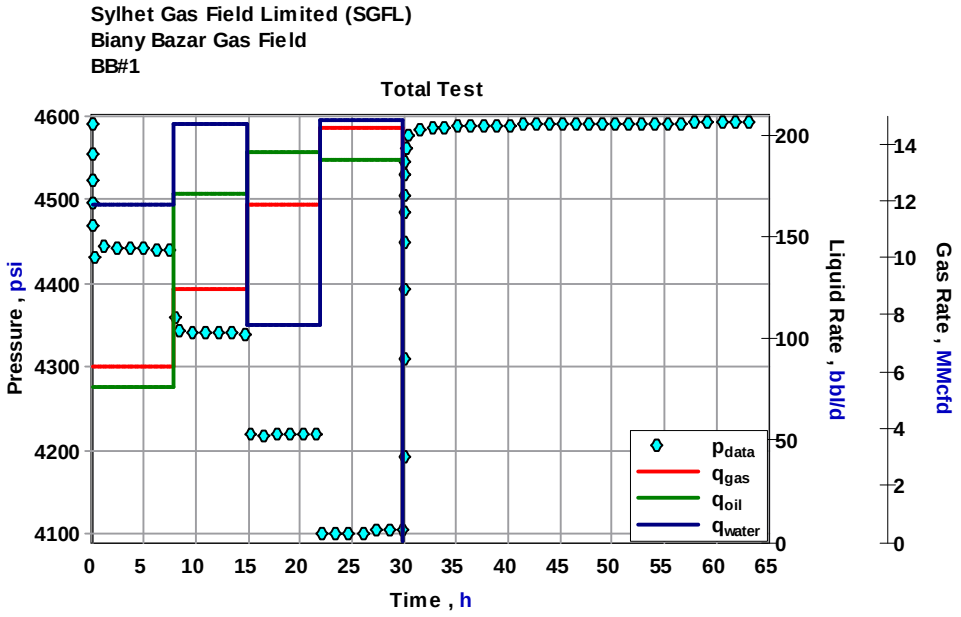

Figure 4.10: Total test data plot of BB # 1

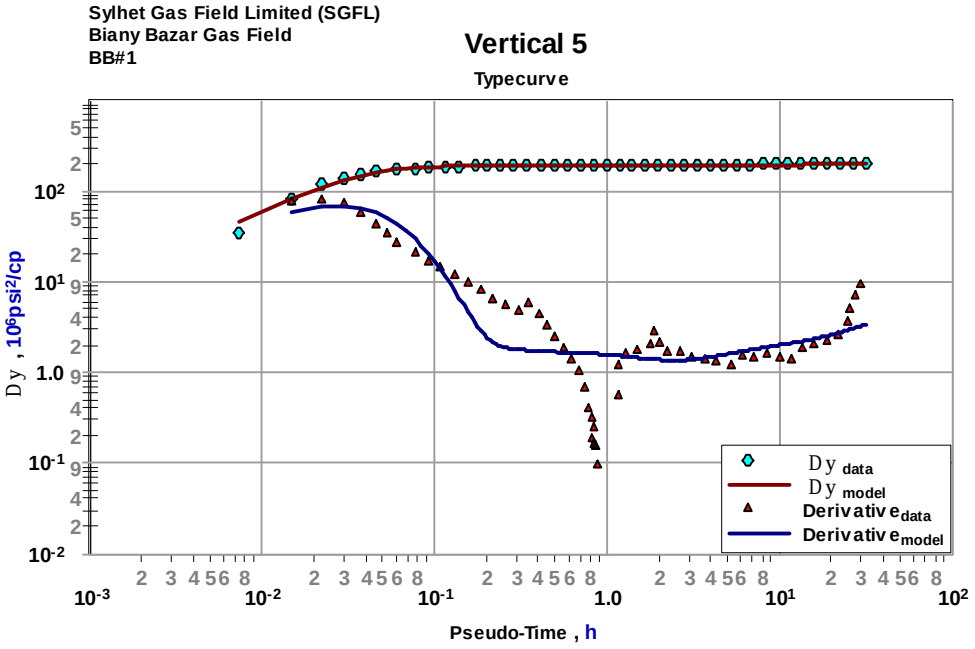

Figure 4.11:Type curve plot of BB # 1

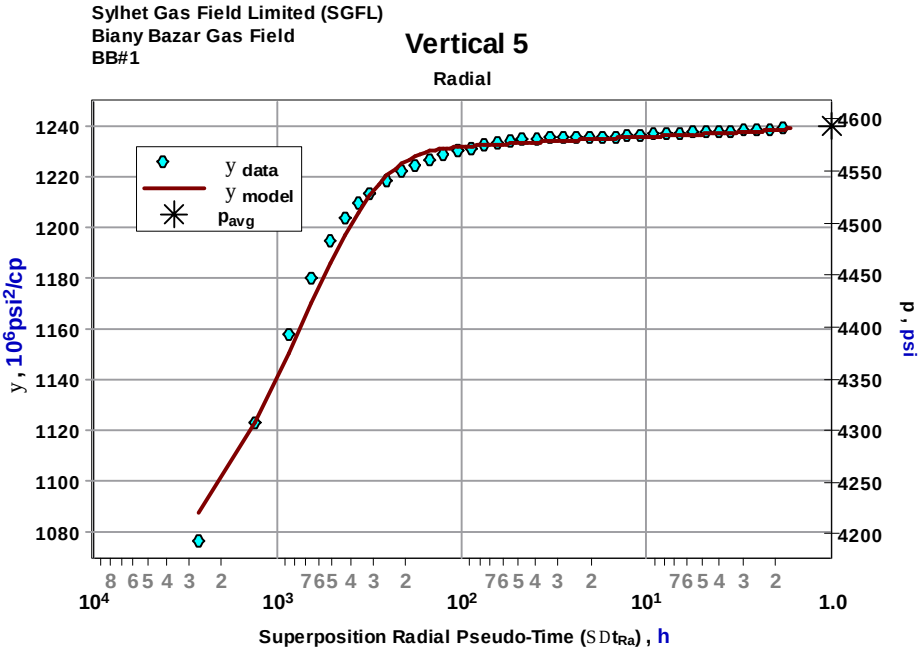

Figure 4.12: Radial analysis and pressure matching of BB # 1

Figure 4.10 shows the variation of flow rates of gas (MMcfd), condensate (bbl/d) and water (bbl/d) with pressure (psia) and time (h). Figure 4.11 shows the type curve matching where variation of difference of pseudo pressure ($\Delta y 10^6$psi^2/cp) and derivative of pseudo

pressure of actual field data with respect to pseudo time (h) are matched with synthetic model data, generated from computer software. Here, near wellbore derivative of pseudo pressure of actual field data shows sudden fall, recommended to further investigation, and late time data shows sudden upward trend. Buildup test should be continued for longer time in future test. Figure 4.12 shows the variation of pseudo pressure ($y10^6$psi^2/cp) with respect to superposition radial pseudo time (h) and, pseudo pressure of actual field data are matched with synthetic model data.

Results

Results of analysis are shown in table 4.8 along with the results of Almansoori and IKM.

Table 4.8: Reservoir/Well Parameters of BB#1 by Different Analysts (Author of this Report, Al-monsure and IKM)

Reservoir/Well Parameters	**Author of This Report**	**Almansoori**	**IKM**
Model Characteristics	**Vertical well**		Wellbore Storage and Skin Homogeneous Closed boundary
Reservoir Parameters			
Total Permeability-thickness Product, kh (md. ft)	13845	2570	21730
Average Permeability, K (md)	213	128.5	201.3
Initial Reservoir Pressure, Pi (Psia)	4613.9	4645	4582
Well and Wellbore Parameters			
WellboreStorage Coefficient, C (bbl/psi)	6.5e-02	0.0234	0.17628
Skin, S	17.1	63.6	33.6

From Table 4.8, it is clear that all Reservoir Parameters and Well and Wellbore Parameters except Initial Reservoir Pressure show dissimilarity. Two main parameters, Average Permeability and Skin, show huge dissimilarity. From core data analysis, Average Permeability of the lower Gas Sand, producing zone of BB#1, is 189.6 md (Table 4.6). Pressure derivative data show a discontinuity near wellbore zone. Almansoori infer retrograde condensation is the cause of this discontinuity near wellbore zone whereas IKM suggested for a little possibility of retrograde condensation. Hence, PVT analysis of reservoir fluid is very important to confirm retrograde condensation.

4.2b BB # 2

BB#2 was completed in the upper gas sand. Total production from May 1999 to October 2007 was 21.08 Bcf from the upper gas sand. Initial total production was 30 MMscf/day from the wells, however, due to increasing water production the daily average production has dropped to 15 MMscf/day. The general tendency has been an increase in water produced and this has been difficult to control. Probable causes could be water coning from an underlying aquifer in both the wells, which might need to be controlled or mitigated (Almansoori). Detailed fluid report has not available, but the fluid is reported to be a gas condensate. This is reasonable because the observed condensate gas ratio at stock tank conditions range from 13 to 20 STB/MMscf. Consequently, it is also expected that a condensate bank may have formed in the vicinity of the wells due to previous production and subsequent well draw down during production testing. It is expected that this will impact the well test analyses. Any information about the dew point pressure or whether this has been reached in the reservoir is not available.

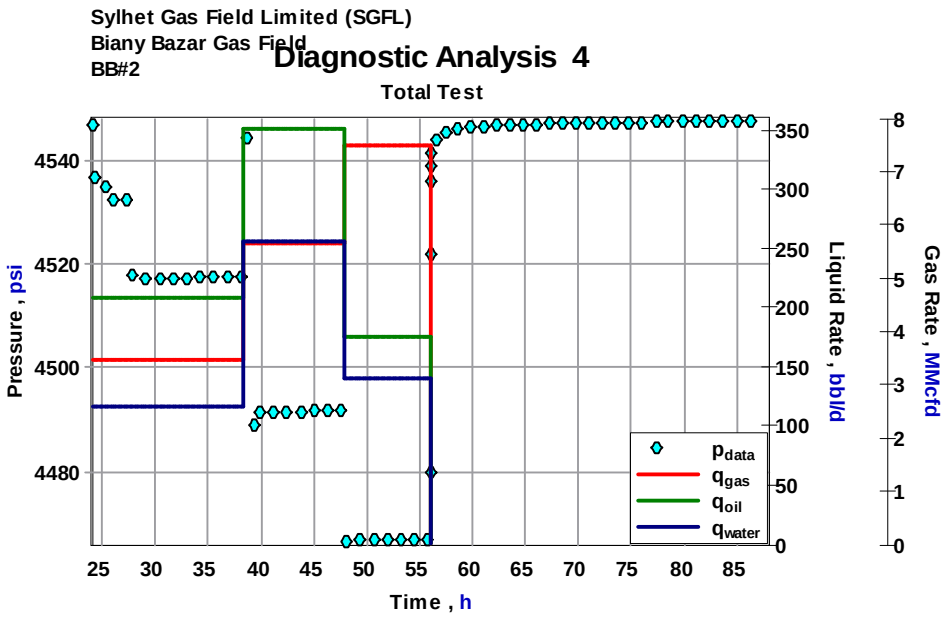

Figure 4.13: Total test data plot of BB # 2

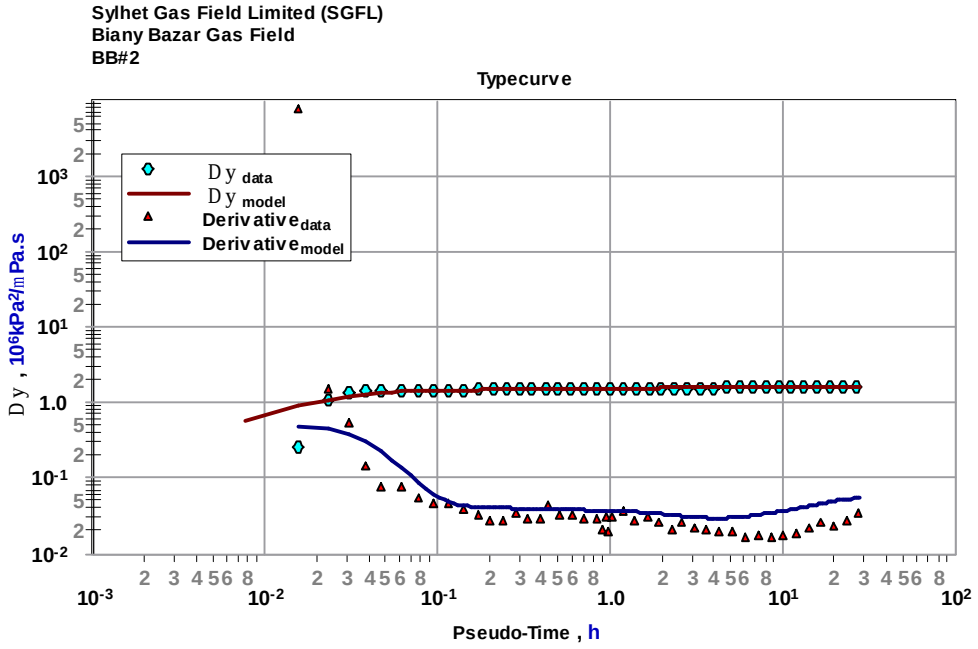

Figure 4.14: Type curve plot of BB # 2

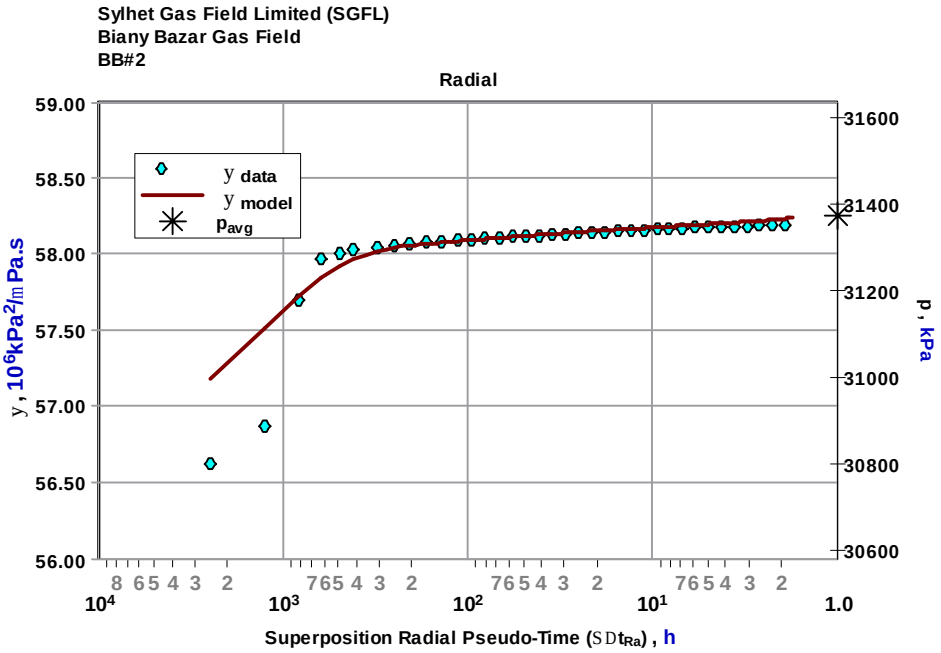

Figure 4.15: Radial analysis and pressure matching of BB # 2

Figure 4.13 shows the variation of flow rates of gas (MMcfd), condensate (bbl/d) and water (bbl/d) with pressure (psia) and time (h). Figure 4.14 shows the type curve matching where

variation of difference of pseudo pressure ($\Delta y 10^6$psi^2/cp) and derivative of pseudo pressure of actual field data with respect to pseudo time (h) are matched with synthetic model data, generated from computer software. Figure 4.15 shows the variation of pseudo pressure ($y 10^6$psi^2/cp) with respect to superposition radial pseudo time (h) and, pseudo pressure of actual field data are matched with synthetic model data.

Results

Results of analysis are shown in table 4.9 along with the results of Almansoori and IKM.

Table 4.9: Reservoir/Well Parameters of (BB#2) by Different Analysts (Author of this Report, Al-monsure and IKM)

Reservoir/Well Parameters	**Author of This Report**	**Almansoori**	**IKM**
Model Characteristics	Vertical		Wellbore Storage and Skin Homogeneous Closed boundary
Reservoir Parameters			
Total Permeability-thickness Product, kh (md. ft)	4971.2	5580	21039
Average Permeability, K (md)	95.6	107.3	204.3
Initial Reservoir Pressure, Pi (Psia)	4552.5	4546.97	4576
Well and Wellbore Parameters			
WellboreStorage Coefficient, C (bbl/psi)	6.5e-02	0.0165	0.17881
Skin, S	13.8	20.9	34.4

Results, shown in Table 4.9, are not varied widely except WellboreStorage Coefficient and Skin. Here, Skin, find out by different analysts, is very high. This high value of positive total skin indicates wellbore damage or mechanical damage. From core data analysis, Average Permeability of the Upper Gas Sand, producing zone of BB#2, is 332.4 md (Table 4.6), which is much higher than that of presented in Table 4.9. Multi phase fluid flow may be the possible cause of this deviation. Relevant data for two phase flow should be collected for future analysis.

4.3 Rashidpur Gas Field

The lithology in the Rashidpur gas reservoir varies and is very complex. The rock is comprised of quartz, feldspars, micas and heavy minerals.

The study of the the Rashidpu field focuses on reserves in two distinct horizons, being the region defined between 4,530 and 4,825 ft kB (4319-4563 ft ss) in the upper sand and 8,880 to 9,145 ft kB (8658-88363 ft ss) in the lower sand of the well R#1.

Rashidpur Gas Field, situated in the hilly area of Habiganj district of Bangladesh, was the highest gas producer field of Sylhet Gas Field. But in course of time production gradually declines there. There are seven producing gas wells. Well no R#1, R#4 and R#7 were available for well testing. Gas produced from Well no R#1, R#4 and R#7 is processed by Silica gel Plant Detail well test diagnosis scenario is presented for Well no R#1, R#4 and R#7 in the following subsection.

Different Producing Sands, Producing Wells and Geo-physical Properties of Biany Bazar Gas Field are shown in following tables.

Table 4.10: Different Producing Sands and Geo-physical Properties of Rashidpur Gas Field

Horizon	Interval (ft KB)	Thickness, h, ft	Average Permeability, k, md (From Core Data Analysis)	Average Porosity, ø, Fraction
Upper Gas Sands	4530-4825	295	370.0	0.25
Lower Gas Sand	8880- 9145	265	-	0.17-0.21

Table 4.11: Different Producing Well and Their Producing Sands of Rashidpur Gas Field

Well	Producing Zone
R#1	Upper Gas Sand
R#4	Upper Gas Sand
R#7	Upper Gas Sand

4.3a R # 1

The intervals tested are three perforation intervals in the Upper Gas Sand from a depth of 4596 ft to 4651 ft, 4661 ft to 4741 ft and 4802 ft to 4809 ft. Condensate gas ratio at stock tank conditions range from 0.20 STB/ MMscf to approximately 0.30 STB/ MMscf. For these values of condensate gas ratio, it may be treated as a dry gas at reservoir conditions (Almansoori). This implies that the gas is not expected to drop condensate in the vicinity of the wellbore during production and there will be no production impairment due to condensate dropout. Production testing for this well was carried out at the Rashidpur station facilities. The well was shut for 2 hours prior to the start of the production test.

Pressure Transient Analysis Plots

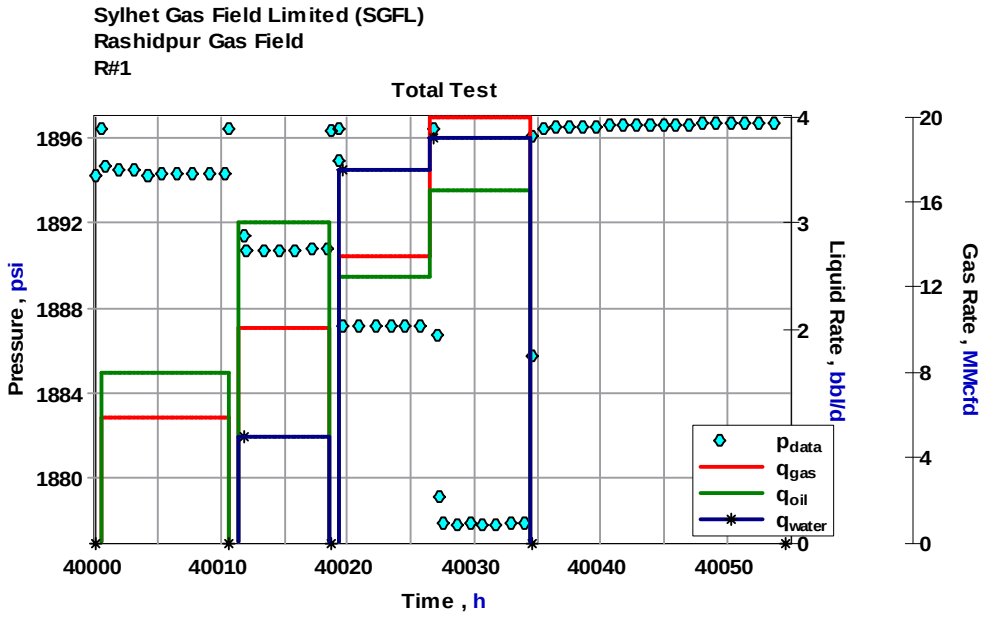

Figure 4.16: Total test data plot of R # 1

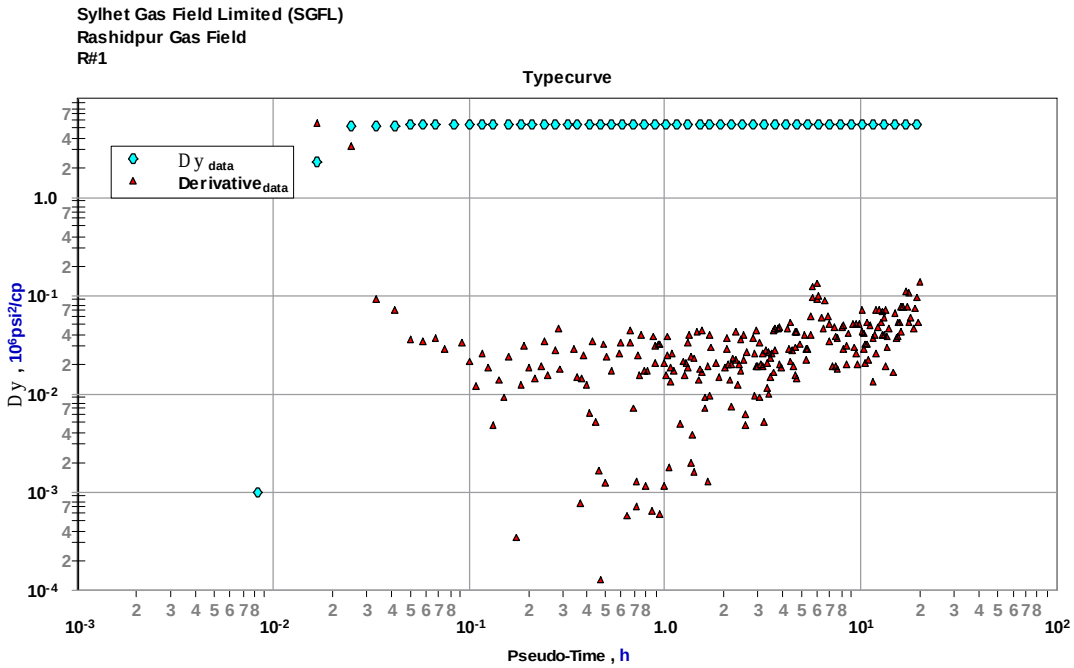

Figure 4.17: Type curve plot of R # 1

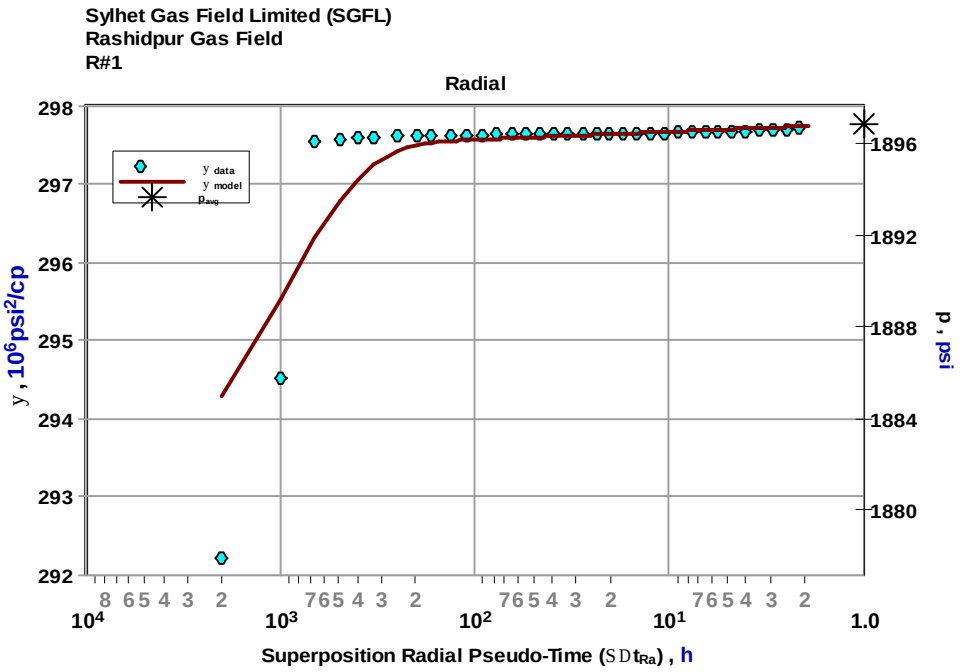

Figure 4.18: Radial analysis and pressure matching of R # 1

Figure 4.16 shows the variation of flow rates of gas (MMcfd), condensate (bbl/d) and water (bbl/d) with pressure (psia) and time (h). Figure 4.17 shows the type curve where variation of difference of pseudo pressure ($\Delta y 10^6$psi^2/cp) and derivative of pseudo pressure of actual field data with respect to pseudo time (h). Here, derivative of pseudo pressure of actual field data are very scattered and, author recommended further analysis to find out cause of scatterings. Figure 4.18 shows the variation of pseudo pressure ($y 10^6$psi^2/cp) with respect to superposition radial pseudo time (h) and, pseudo pressure of actual field data are matched with synthetic model data.

Results

Results of analysis are shown in table 4.12 long with the results of Almansoori and IKM.

Table 4.12: Reservoir/Well Parameters of (R#1) by Different Analysts (Author of this Report, Al-monsure and IKM)

Reservoir/Well Parameters	**Author of This Report**	**Almansoori**	**IKM**
Model Characteristics	Vertical	Standard with Constant Wellbore Storage	Wellbore Storage and Skin Homogeneous
Reservoir Parameters			
Total Permeability-thickness Product, kh (md ft)	3.1e+05	5.77e+05	1218007
Average Permeability, K (md)	2150	4063	3930
Initial Reservoir Pressure, Pi (Psia)	1897.1	1896	2055.6
Well and Wellbore Parameters			
WellboreStorage Coefficient, C (bbl/psi)	2.98	1.3	0.229
Skin, S	7.20	50.2	544.8

From Table 4.12, it is clear that all Reservoir Parameters and Well and Wellbore Parameters except Initial Reservoir Pressure show dissimilarity. However, from core data analysis, Average Permeability of the Upper Gas Sand, producing zone of R# 1, is 370.0 md (Table 4.10). Two main parameters, Average Permeability and Skin, show huge dissimilarity. Specially, Skin varies widely. Besides, Pressure derivative data, in figure 4.17, is very scattered and, late time Pressure derivative data shows a sudden upward trend (+1/2 slope line), which indicates that the well might be within a channel. High value of skin indicates extra pressure drop near wellbore due to wellbore damage. Further analysis is necessary for better results.

4.3b R # 4

The intervals tested are two perforation intervals in the Upper Gas Sand from a depth of 9144 ft to 9164 ft and Lower Gas Sand from a depth of 9180 ft to 9200 ft respectively. The condensate gas ratio values reported during the production test is 0.5 STB/ MMscf. While this value is high and the condensate can be treated as a wet gas, there is evidence of a radial composite behavior in the well test analysis. This implies that the gas might have dropped condensate in the vicinity of the wellbore during previous production periods thereby causing production impairment. It is also possible that the near wellbore region might be damaged to a certain distance from the wellbore. It is not possible to distinguish between these 2 effects (Almansoori). Production testing for this well was carried out at the Rashidpur station process plant separator located 6 km away from the well.

Pressure Transient Analysis Plots

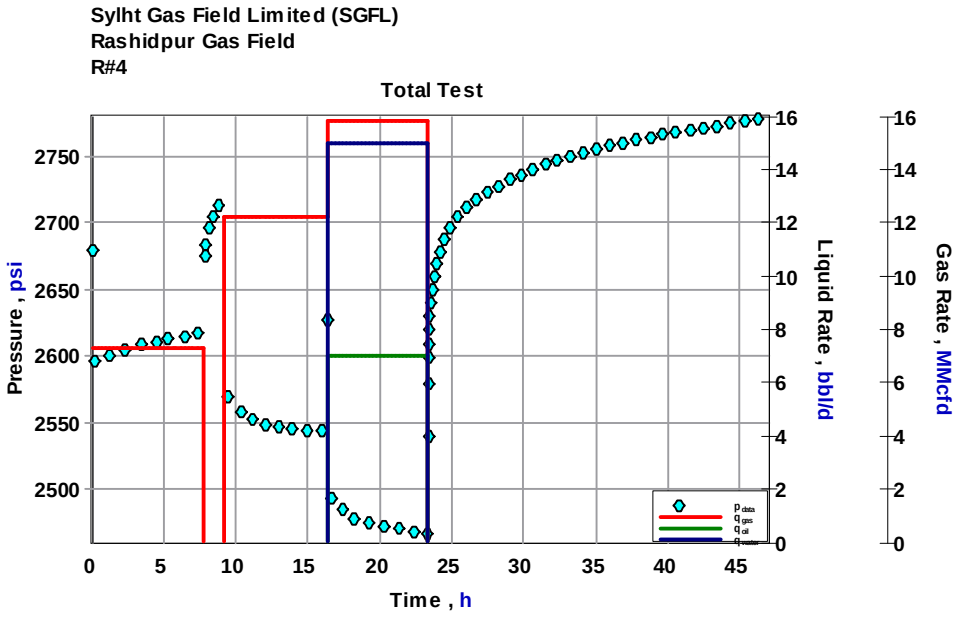

Figure 4.19: Total test data plot of R # 4

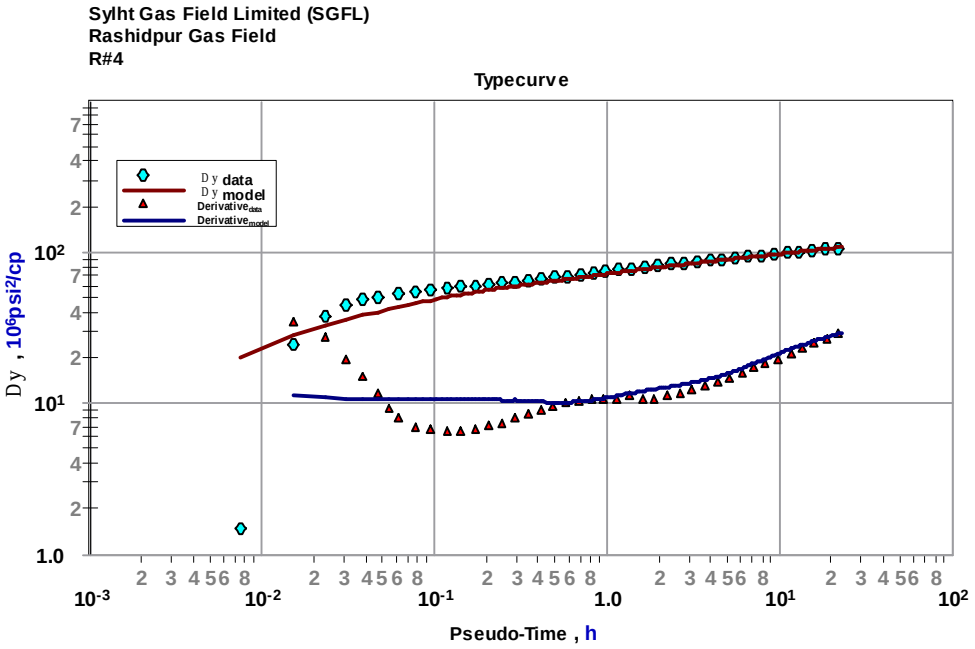

Figure 4.20: Type curve plot of R # 4

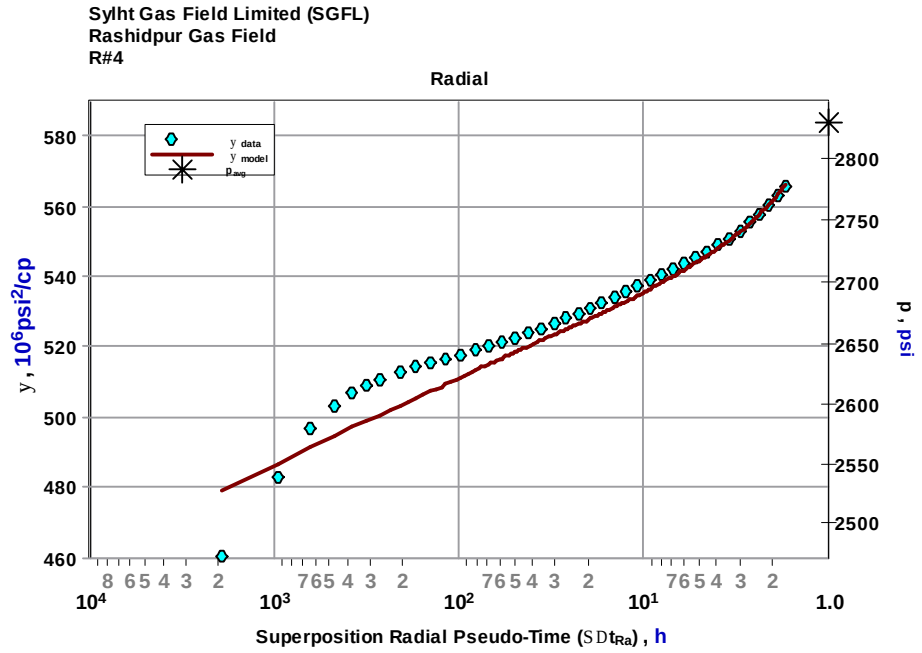

Figure 4.21: Radial analysis and pressure matching of R # 4

Figure 4.19 shows the variation of flow rates of gas (MMcfd), condensate (bbl/d) and water (bbl/d) with pressure (psia) and time (h). Figure 4.20 shows the type curve matching where variation of difference of pseudo pressure ($\Delta y 10^6 psi^2/cp$) and derivative of pseudo pressure of actual field data with respect to pseudo time (h) are matched with synthetic model data, generated from computer software. Figure 4.21 shows the variation of pseudo pressure ($y 10^6 psi^2/cp$) with respect to superposition radial pseudo time (h) and, pseudo pressure of actual field data are matched with synthetic model data. Here, matching of synthetic model data with actual field data is excellent.

Results

Results of analysis are shown in table 4.13 along with the results of Almansoori and IKM.

Table 4.13: Reservoir/Well Parameters of (R#4) by Different Analysts (Author of this Report, Al-monsure and IKM)

Reservoir/Well Parameters	**Author of This Report**	**Almansoori**	**IKM**
Model Characteristics	Vertical	Standard with Changing Wellbore Storage	Wellbore Storage and Skin Homogeneous Sealing boundary
Reservoir Parameters			
Total Permeability-thickness Product, kh (md. ft)	640	995	698.1
Average Permeability, K (md)	16	25	11.6
Initial Reservoir Pressure, Pi (Psia)	2782.1	2776	3987.4
Well and Wellbore Parameters			
WellboreStorage Coefficient, C (bbl/psi)	2.98	0.0063	0.00945
Skin, S	-4.80	-2	-0.29

Results, shown in Table 4.5, are not varied widely. However, from core data analysis, Average Permeability of the Upper Gas Sand, producing zone of R# 4, is 370.0 md (Table 4.10). Here, lower value of Average Permeability indicates tight reservoir whereas negative value of Skin indicates wellbore improvement due to natural fracture or other causes.

4.3c R # 7

The interval tested is at a depth of 9123 ft to 9149 ft in the Upper Gas Sand. The condensate gas ratio at stock tank conditions ranged from 1.0 STB/ MMscf to 0.8 STB/ MMscf during the test. For this value of condensate gas ratio, it may be treated as a wet gas at reservoir conditions (Almansoori). However, there is some evidence of a higher skin zone close to the wellbore and this may be due to condensate dropout or other reasons like formation damage. Production testing for this well was carried out at the Rashidpur station facilities located 11 km away from the well.

Pressure Transient Analysis Plots

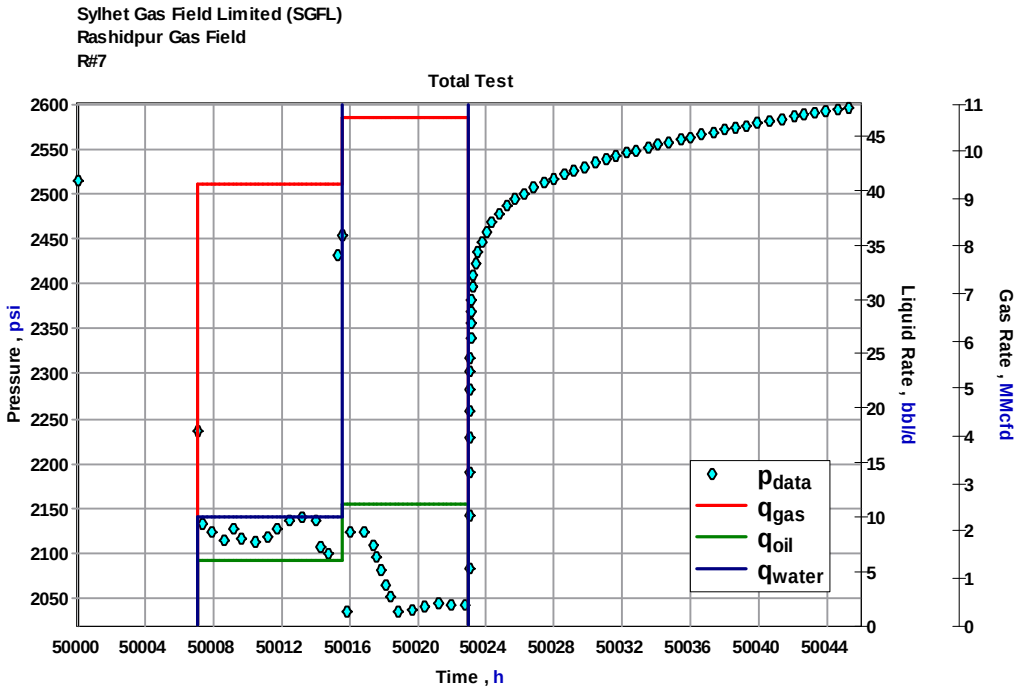

Figure 4.22: Total test data plot of R # 7

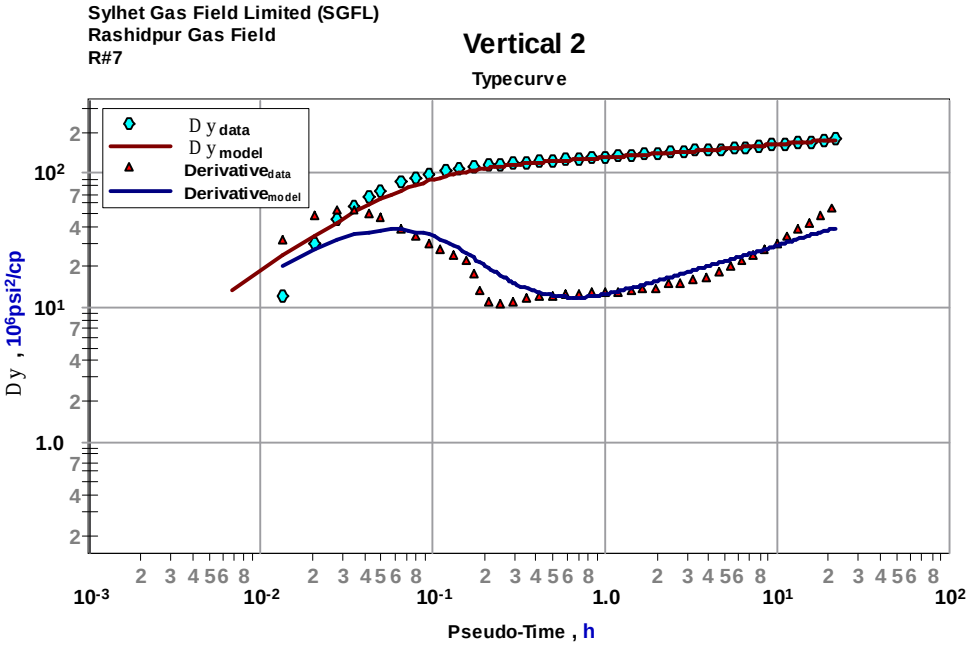

Figure 4.23: Type curve plot of R # 7

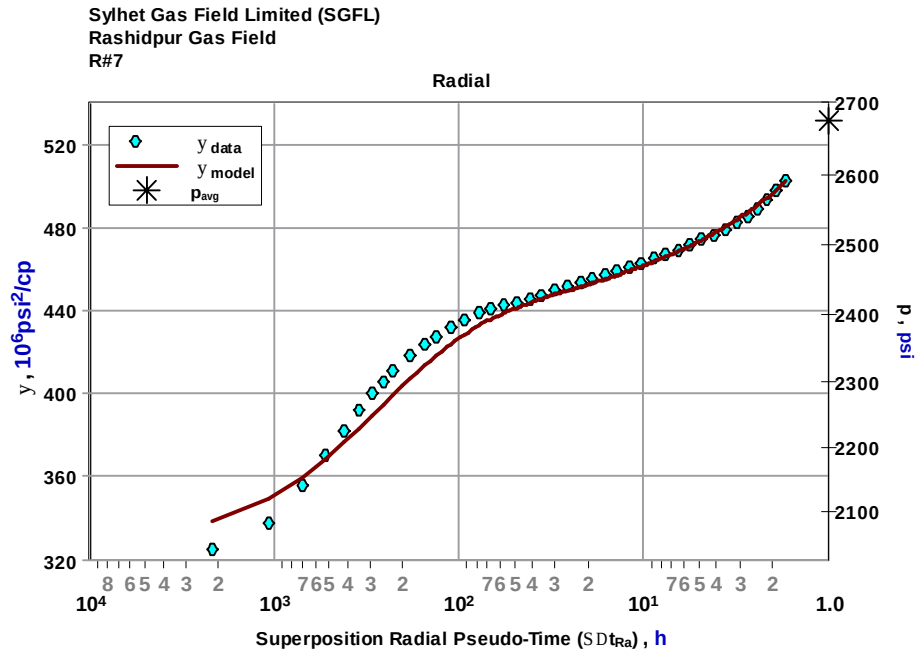

Figure 4.24: Radial analysis and pressure matching of R # 7

Figure 4.22 shows the variation of flow rates of gas (MMcfd), condensate (bbl/d) and water (bbl/d) with pressure (psia) and time (h). Figure 4.23 shows the type curve matching where variation of difference of pseudo pressure ($\Delta y 10^6 psi^2/cp$) and derivative of pseudo pressure of actual field data with respect to pseudo time (h) are matched with synthetic model data, generated from computer software. Figure 4.24 shows the variation of pseudo pressure ($y 10^6 psi^2/cp$) with respect to superposition radial pseudo time (h) and, pseudo pressure of actual field data are matched with synthetic model data. Here, matching of synthetic model data with actual field data is excellent.

Results

Results of analysis are shown in table 4.14 along with the results of Almansoori and IKM.

Table 4.14: Reservoir/Well Parameters of (R#7) by Different Analysts (Author of this Report, Al-monsure and IKM)

Reservoir/Well Parameters	**Author of This Report**	**Almansoori**	**IKM**
Model Characteristics	Vertical	Standard with Constant Wellbore Storage	Not Available
Reservoir Parameters			
Total Permeability-thickness Product, kh (md. ft)	540.8	450	
Average Permeability, K (md)	20.8	17.3	
Initial Reservoir Pressure, Pi (Psia)	2610.7	2621	
Well and Wellbore Parameters			
WellboreStorage Coefficient, C (bbl/psi)	0.07	0.031	
Skin, S	-0.70	0.4	

Results, shown in Table 4.14, are not varied widely. However, from core data analysis, Average Permeability of the Upper Gas Sand, producing zone of R# 7, is 370.0 md (Table 4.10). Here, lower value of Average Permeability indicates tight reservoir whereas negative value of Skin indicates wellbore improvement due to natural fracture or other causes.

CHAPTER 5

Deliverability Test

Deliverability test is performed to measure the performance of a gas well because it quantifies the ability of a reservoir to deliver gas to the wellbore. Deliverability tests make possible the prediction of flow rates against any particular back pressure, including AOF when the back pressure is zero. Deliverability test results are important to producing and transporting companies in the preparation of field development programs, in the design of gathering and pipeline facilities, in the design of processing plants, and in the negotiation of gas sale contracts. In this chapter deliverability of different wells are determined.

Conventional Backpressure Test

Predicting the inflow performance of gas wells is a process that has relied almost exclusively on some form of multipoint well testing procedure. The conventional backpressure or flow-after-flow test, isochronal test, and modified isochronal test have been used to predict the deliverability of gas wells. Rawlins and Schellhardt (1936) presented the back-pressure method of testing gas wells. It is dependent upon the requirement that a series of flow rates and corresponding pressure data be obtained under stabilized flow conditions. The conventional backpressure equation is given by:

$$q_{st} = C\left(\bar{p}_R{}^2 - p_{wf}{}^2\right)^n \equiv C(\Delta p^2)^n \quad \text{.....(2.1)}$$

where:

q_{st} = flow rate at standard conditions, MMscfd

$\bar{p}_R$ = average reservoir pressure obtained by shut-in of the well to complete stabilization, psia

p_{wf} = flowing sandface pressure, psia

Δp^2 = $\left(\bar{p}_R{}^2 - p_{wf}{}^2\right)^n$

C = a coefficient which describes the position of the stabilized deliverability line

n = an exponent which describes the inverse of the slope of the stabilized deliverability line

These data are plotted on logarithmic coordinates of the difference in the pressures squared versus the flow rate in order to determine the constants, C, and, n. Once C and n are

determined, flow rates can be estimated as a function of flowing bottomhole pressure. The method of testing was applicable for those wells which approached stabilized producing conditions within a relatively short period of time. Stabilized performance characteristics could not be determined by this method for wells that approached stabilized producing conditions slowly, which usually occur in lower permeability reservoirs. To overcome slow stabilization, Cullender (1955) proposed the isochronal test method of determining the flow characteristics of gas wells. Cullender used the term "isochronal" because only those conditions existing as a result of a single disturbance of constant duration are considered. The expression "single disturbance of constant duration" is intended to define those conditions existing around a well as a result of a constant flow rate existing for a specific period of time from shut-in conditions. Cullender developed an empirical method whereby the deliverability exponent, n, of the back pressure curve may be determined for a particular gas well. Once the deliverability exponent is determined, the characteristic slope is applied to an extended stabilized flow point to determine the deliverability coefficient C. Although Cullender's method was an improvement, it still had the drawback of extended shut in periods to reach the stabilized pressure before each flow period. To overcome extended shut in periods to reach the stabilized pressure, Katz (1959) 1introduced the modified isochronal test method. Katz proposed flow periods of equal length and shut-in periods between flow periods of equal length followed by an extended, stabilized flow point and shut-in period. Once the data is obtained, it is analyzed in a manner very similar to Cullender, with the deliverability exponent determined from the transient test data, which is then applied to the extended, stabilized flow data to determine the deliverability coefficient

Absolute Open Flow (AOF)

The absolute open flow (AOF) potential of a well is the rate at which the well would produce against zero sandface back pressure. It is used as a measure of gas well performance because it quantifies the ability of a reservoir to deliver gas to the wellbore.

Types of Deliverability Tests

There are a number of tests which can be conducted in order to calculate the deliverability of a well as described below.

Conventional Back Pressure Test

The conventional back pressure test is conducted by flowing a well at different rates. Each rate is sustained until the radius of investigation has reached the outer edge of the drainage area and pressure stabilization has been reached. This type of test is not practical for low permeability reservoirs because the time to reach pressure stabilization for each rate is excessive.

Isochronal Test

A fundamental reason that the conventional test is theoretically sound is that the radius of investigation is constant for each flow period. In order to uphold this principle, the isochronal test takes advantage of the fact that the radius of investigation is a function of time and not flow rate. An isochronal test is conducted by flowing a well at several different flow rates for periods of equal duration, normally much less than the time required for stabilization. A shut-in, long enough for the pressure to reach essentially static conditions, is performed between each flow period. In addition, an extended flow rate, long enough to reach pressure stabilization, is required. In tight reservoirs the length of time required to reach pressure stabilization between flow periods could make the isochronal test impractical.

Modified Isochronal Test

The modified isochronal test is an isochronal test which requires that each shut-in between flow periods, rather than being long enough to attain essentially static conditions should be of the same duration as each flow period. It also requires an extended flow period.

Single Point Test

A single point test consists only of an extended flow period. They require an estimate of the degree of turbulent flow in the formation. This estimate is often based on information provided by other wells in the same formation or calculated from reservoir and fluid properties**.**

AOF Flow Conditions

Extended Flow

Normally an isochronal test includes one flow rate that is extended to stabilization and a stabilized pressure and flow rate point is determined. This point is the extended flow pressure and flow rate for the test. Single point tests do not include the multi-rate portion of a test and consist of only an extended rate and pressure.

Stabilized Shut-in

Stabilized generally refers to a test in which the pressure no longer changes significantly with time. For AOF tests, the stabilized shut-in pressure is a pressure that reflects the average reservoir pressure at the time. It is either measured during the test or determined from the interpretation of the data.

Stabilized Flow

In high permeability reservoirs or wells with small drainage areas, it may be possible to flow the well until stabilization during the extended flow period of a deliverability test. In these cases, the stabilized pressure and flow rate point is the extended flow point. Any tests, however, are not flowed to stabilization because of time constraints (especially in tight reservoirs). An extended flow and stabilized shut-in are still performed at the end of these deliverability tests so that the buildup data can be analyzed and from that the stabilized rate calculated. Stabilized flow can be determined by calculation or by creating a model of the reservoir, doing a forecast at a specified pressure, and finding the point when the rate has stabilized (usually at 3 months, 6 months, or 1 year) .\

Types of Analyses

Two types of analysis are available, the simplified analysis or the laminar-inertial-turbulent (LIT) analysis. LIT analysis is more rigorous than simplified analysis and is usually only used in tests where turbulence is dominant and the extrapolation to the AOF is large. However, in most cases the simplified analysis is sufficient to determine the AOF and deliverability. For both the simplified and LIT analysis, two pressure options are available,

the pressure squared or the pseudo-pressure approach. Here, the simplified analysis is used to determine the AOF and deliverability.

Pressure Squared

The pressure squared approach is the more traditional method, and is often used because it is easier to understand and calculate. However, it is only valid for medium to low pressure ranges but is just as accurate as the pseudo-pressure approach in this range.

Pseudo-Pressure

Using pseudo-pressure will be more accurate than the pressure squared approach, especially when dealing with a high pressure system, where gas viscosity (μ) and compressibility (c) cannot be assumed to be constant. Thus, pseudo-pressure works for all pressure ranges, although it is more difficult to calculate and requires more computational time.

Simplified Analysis

The simplified analysis is based on the following equation:

Pressure squared

$$q_{st} = C\left(\overline{p}_R{}^2 - p_{wf}{}^2\right)^n$$

Pseudo-pressure

$$q_{st} = C\left(y_R{}^2 - y_{wf}{}^2\right)^n$$

For the modified isochronal test, p_{ws} must be used instead of $\overline{p}_R$ because the duration of each shut-in period is too short to reach static conditions.

The data is plotted on a log-log plot of Δp^2 versus q_{st} where Δp^2 is defined as:

$$\Delta p^2 = \left(p_{ws}{}^2 - p_{wf}{}^2\right)^n$$

The flow and shut-in periods of equal duration provide the information required to plot the points. A straight line, called the transient deliverability line, is drawn through these points. The duration of the last flow rate is extended until the pressure response has stabilized. This information is used to plot another point called the stabilized point. A line parallel to the

transient deliverability line is drawn through the stabilized point. This is called the stabilized deliverability line. If the extended flow period does not reach pressure stabilization, a stabilized point can be found by calculation from a buildup test.

The parameter n can be determined from the slope of the line as follows:

$$q_{st} = C\left(\bar{p}_R{}^2 - p_{wf}{}^2\right)^n$$

$$\log(q_{st}) = \log C + n.\log\left(\bar{p}_R{}^2 - p_{wf}{}^2\right)$$

$$\log\left(\bar{p}_R{}^2 - p_{wf}{}^2\right) = \frac{1}{n}\log(q_{st}) - \frac{1}{n}\log C$$

Thus, slope is equal to 1 / n, and n is called the inverse slope.

The other parameter, C, can be determined using n and the coordinates (q_{st} and $\bar{p}_R$) of any point on the stabilized deliverability line (e.g. the stabilized point) as follows:

$$C = \frac{q_{st}}{\left(\bar{p}_R{}^2 - p_{wf}{}^2\right)^n}$$

Performance Coefficient C and Exponent n

The Performance Coefficient C can be regarded as an intercept equal to q when the difference of the squared-pressure terms equals unity. For high-permeability gas wells that stabilize rapidly, C does not change significantly with time. Hence, the initial back pressure curve can be used to approximate the flow capacity during the life of the well within reasonable accuracy. Actually the Performance Coefficient, C, will change with pressure and flow rate.

In low-permeability reservoirs, the rate of gas production during relatively short flow periods decreases with time at a fixed flowing wellhead pressure. Likewise, the value of C decreases with time during short flow periods. Wells with these characteristics have a series of back-pressure curves with time of flow as a parameter.

Generally, the value of the exponent n ranges from 0.5to1.0. Low-permeability gas wells will normally yield bottom hole back-pressure curves with n values more nearly approaching 1.0, while high-permeability gas wells yield n values more nearly approaching 0.5. Under near-steady state conditions, the exponent 0.5 and 1.0 represent turbulent and laminar flow in porous media, respectively.

Generally, the slope of the back-pressure plot is an indication of wellbore and skin damage. n=1 (Q= 45º) implies little or no wellbore and skin damage. As n decreases towards 0.5 (Q decreases towards 26.5º), wellbore and skin damage increases. if n is outside the range 0.5to 1 , well test data may be erroneous because of insufficient cleanup or liquid loading in the gas well (Ikoku. Chi U. , 1992).

Note that C and n are considered to be constant for a limited range of flow rates. In theory, it is expected that this form of the deliverability relationship will be used only for the range of flow rates used during the test. However, in practice it is used indiscriminately for a wide range of rates and pressures.

The absolute open flow (AOF) potential, The Performance Coefficient C and Exponent n of different wells is determined in the next section.

5.1a KTL#1

Here, 3 draw down data, (11.0782 MMscfd, 3453 psia), (16.22 MMscfd, 3465 psia) and (18.8 MMscfd, 3440 psia), are used to find out absolute open flow (AOF) potential. Shut-in pressure P_{WS}, 3503.0, found by buildup analysis, is taken as P_R. Extended flow data should have measured during the test. Hence, IPR/deliverability curve dose not represent the correct AOF and C. But value of n is not affected by this as the slope of the line is indicated by 1/n.

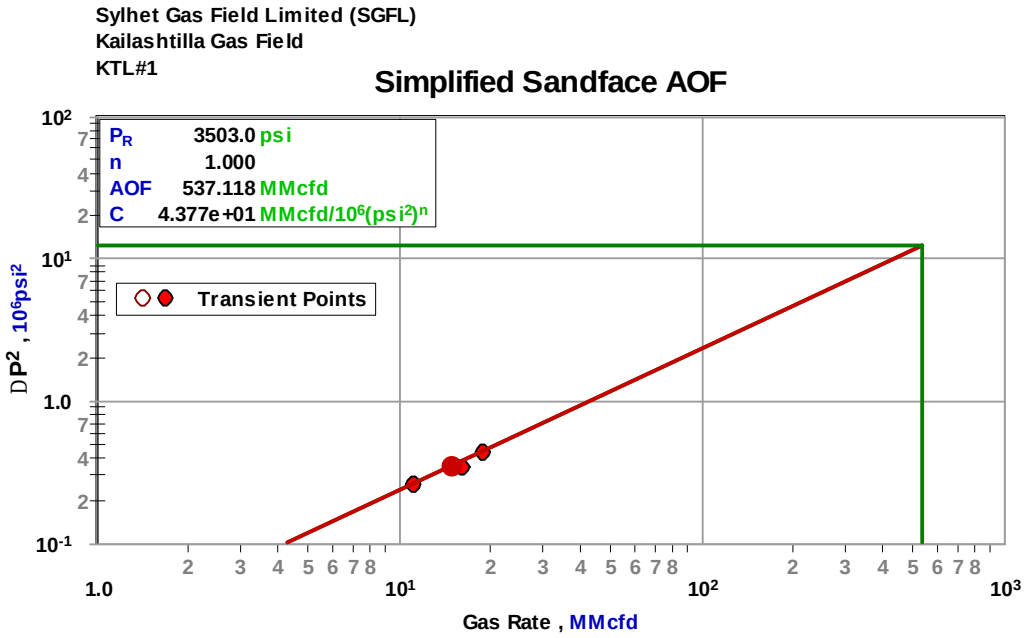

Figure 5.1: Deliverability line of KTL # 1

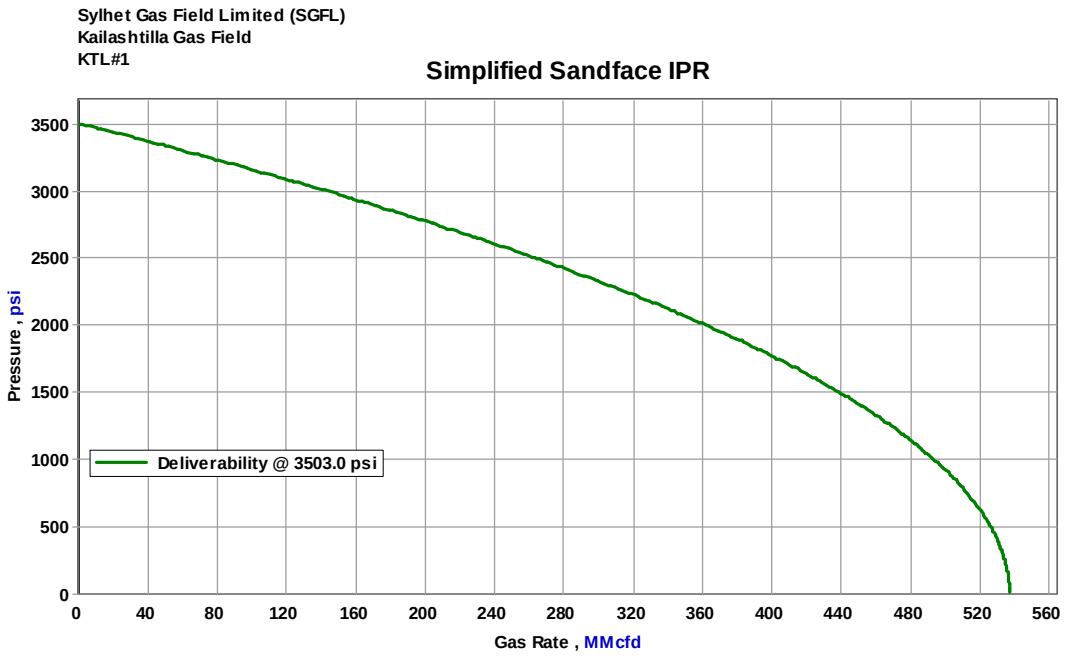

Figure 5.2: IPR curve of KTL # 1

Absolute Open Flow (AOF) Test Review

The major parameters that are found in Back Pressure Test are AOF=537.12 MMcfd, n=1 and C=4.38e+01 MMcfd/10 ^{6} $(psi^{2})^{n}$.

5.1b KTL#2

Here, 3 draw down data, (4 8.976 MMscfd, 3215 psia), (15.81 MMscfd, 3211psia) and (24.125 MMscfd, 3205psia), are used to find out absolute open flow (AOF) potential. Shut-in pressure P_{WS}, 3233, found by buildup analysis, is taken as P_R. Extended flow data should have measured during the test. Hence, IPR/deliverability curve dose not represent the correct AOF and C. But value of n is not affected by this as the slope of the line is indicated by 1/n.

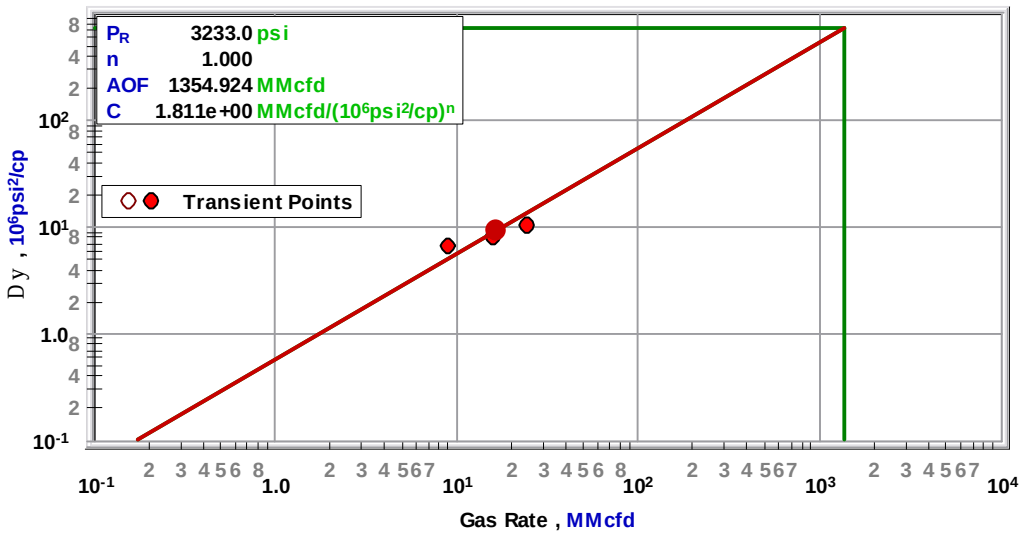

Figure 5.3: Deliverability line of KTL # 2

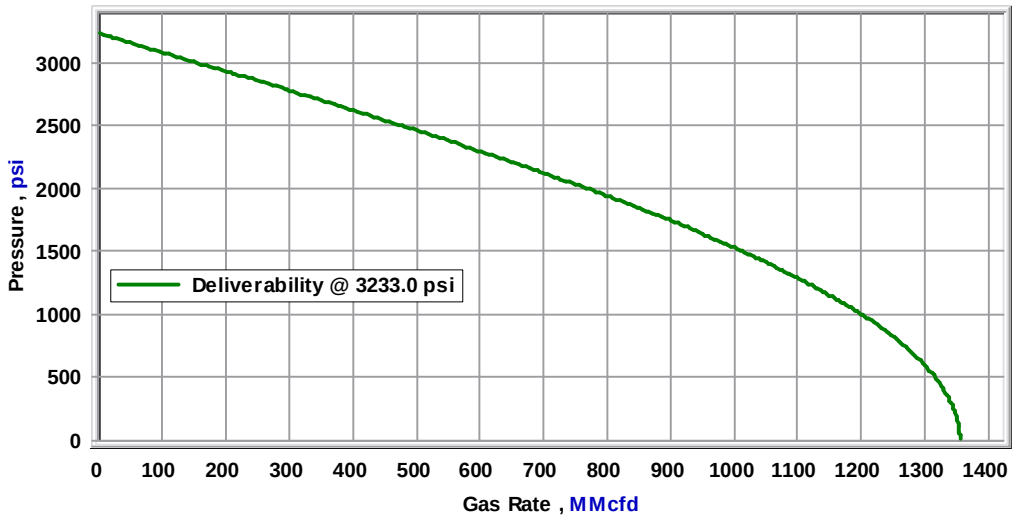

Figure 5.4: IPR curve of KTL # 2

Absolute Open Flow (AOF) Test Review

The major parameters that are found in Back Pressure Test are AOF=1354.92 MMcfd, n=1.00 and C=1.811e+0 MMcfd/10 ^{6} $(psi^2)^n$.

5.1c KTL #4

Here, 2draw down data, (14.2 MMscfd, 3452psia) and (18.389 MMscfd, 3437psia), are used to find out absolute open flow (AOF) potential. Shut-in pressure P_{WS}, 3495, found by buildup analysis, is taken as P_R. Extended flow data should have measured during the test. Hence, IPR/deliverability curve dose not represent the correct AOF and C. But value of n is not affected by this as the slope of the line is indicated by 1/n.

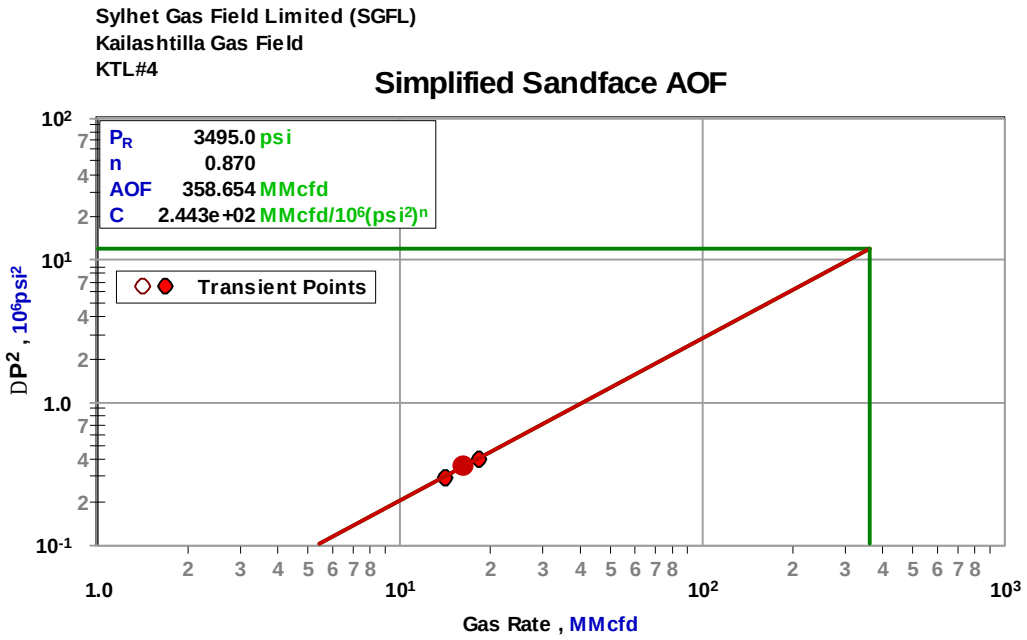

Figure 5.5: Deliverability line of KTL # 4

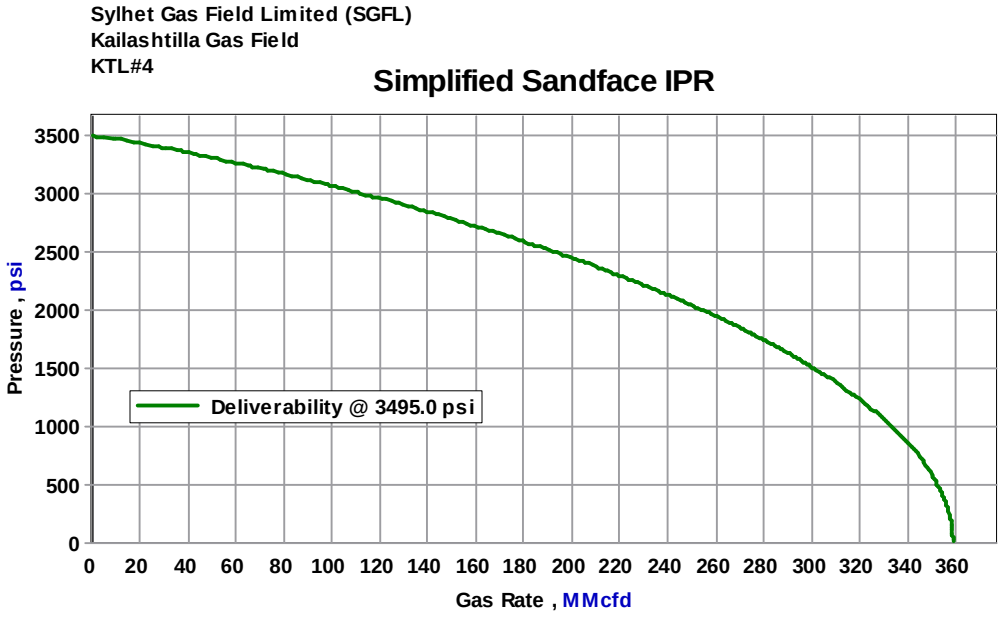

Figure 5.6: IPR curve of KTL # 4

Absolute Open Flow (AOF) Test Review

The major parameters that are found in Back Pressure Test are AOF=358.6 MMcfd, n=0.870 and C=2.44e+02 MMcfd/10 ^{6} $(psi^2)^n$.

5.2a BB#1

Here, 4 draw down data, (6.16 MMscfd, 4440 psia), (8.824 MMscfd, 4339 psia), (11.77 MMscfd, 4220 psia) and (14.468 MMscfd, 4104 psia), are used to find out absolute open flow (AOF) potential. Shut-in pressure P_{WS}, 4614, found by buildup analysis, is taken as P_R. Extended flow data should have measured during the test. Hence, IPR/deliverability curve dose not represent the correct AOF and C. But value of n is not affected by this as the slope of the line is indicated by 1/n.

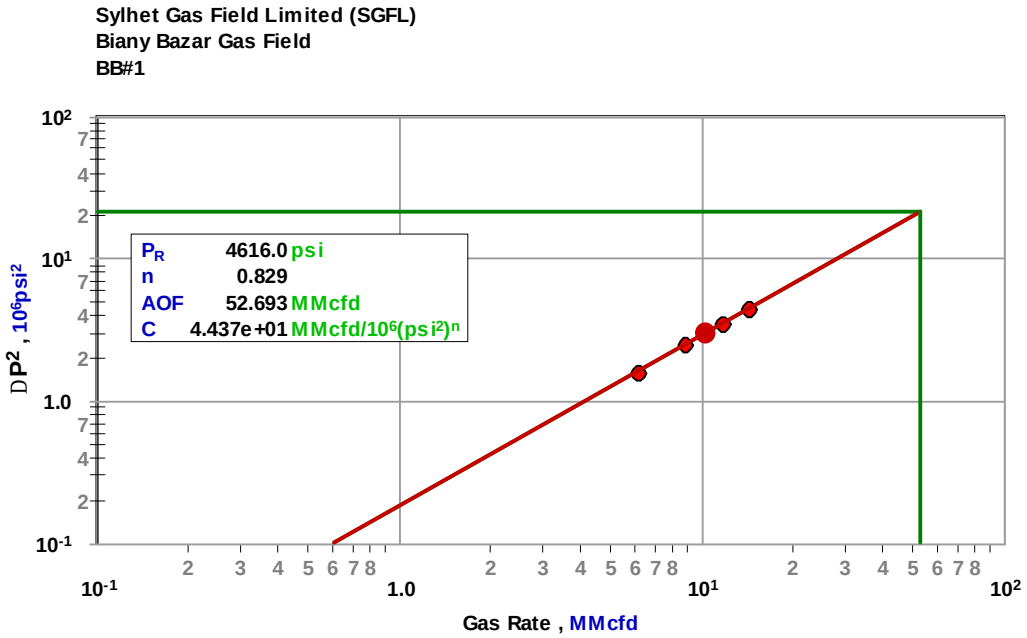

Figure 5.7: Deliverability line of BB # 1

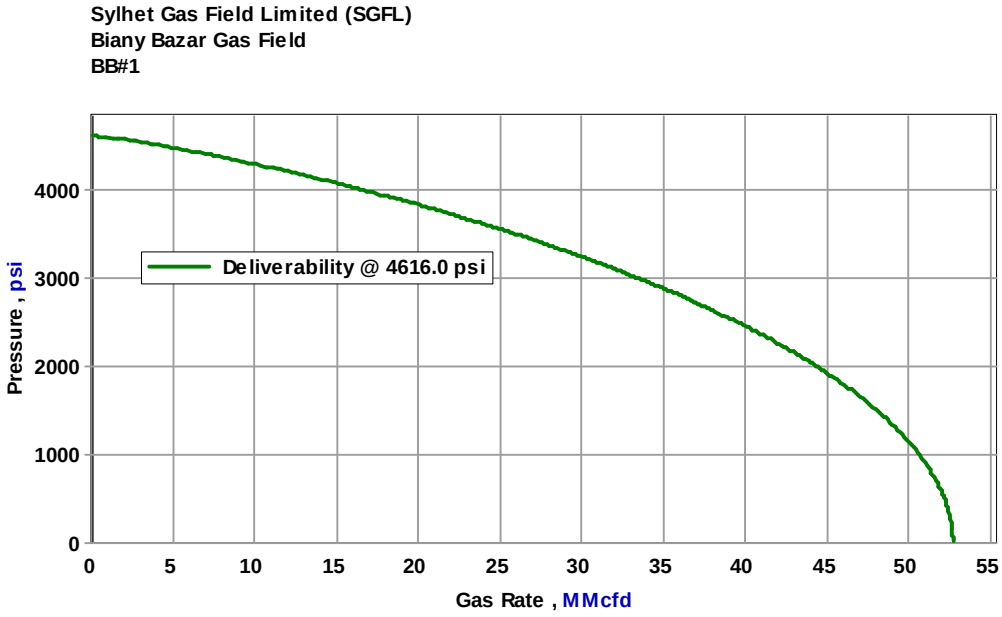

Figure 5.8: IPR curve of BB # 1

Absolute Open Flow (AOF) Test Review

The major parameters that are found in Back Pressure Test are AOF=52.69 MMcfd, n=0.829 and C=4.437e+01 MMcfd/10 ^{6} $(psi^{2})^{n}$.

5.2b BB # 2

Here, 3 draw down data, (3.44 MMscfd, 4517psia), (5.616 MMscfd, 4491.6psia) and (7.429 MMscfd, 467psia), are used to find out absolute open flow (AOF) potential. Shut-in pressure P_{WS}, 4552, found by buildup analysis, is taken as P_R. Extended flow data should have measured during the test. Hence, IPR/deliverability curve dose not represent the correct AOF and C. But value of n is not affected by this as the slope of the line is indicated by 1/n.

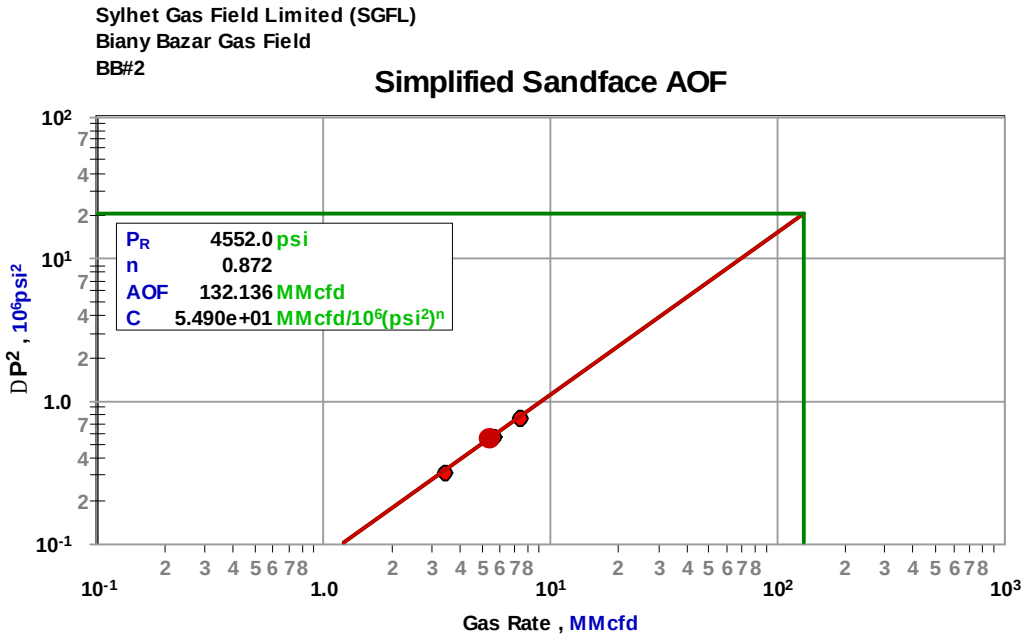

Figure 5.9: Deliverability line of BB # 2

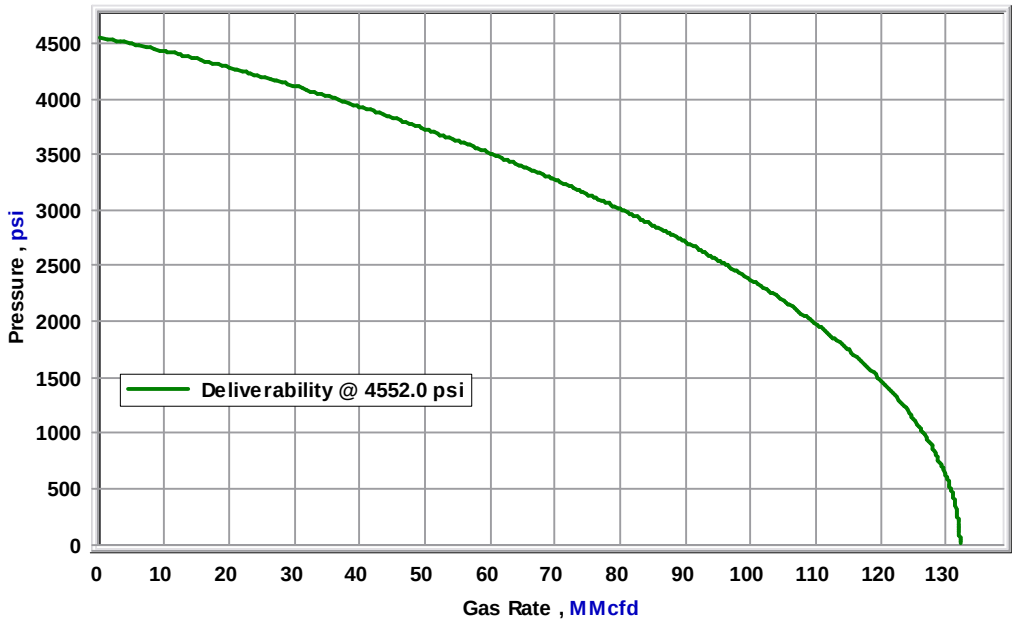

Figure 5.10: IPR curve of BB # 2

Absolute Open Flow (AOF) Test Review

The major parameters that are found in Back Pressure Test are AOF=132.136 MMcfd, n=0.872 and C=5.49e+01 MMcfd/10 ^{6} $(psi^2)^n$.

5.3a R # 1

Here, 4 draw down data,(5.818 MMscfd, 1894 psia) (10.093 MMscfd, 1890.7 psia), (13.413 MMscfd, 1887.2 psia) and (19.984, 1877.9), are used to find out absolute open flow (AOF) potential. . Shut-in pressure P_{WS}, 1897, found by buildup analysis, is taken as P_R. Extended flow data should have measured during the test. Hence, IPR/deliverability curve dose not represent the correct AOF and C. But value of n is not affected by this as the slope of the line is indicated by 1/n.

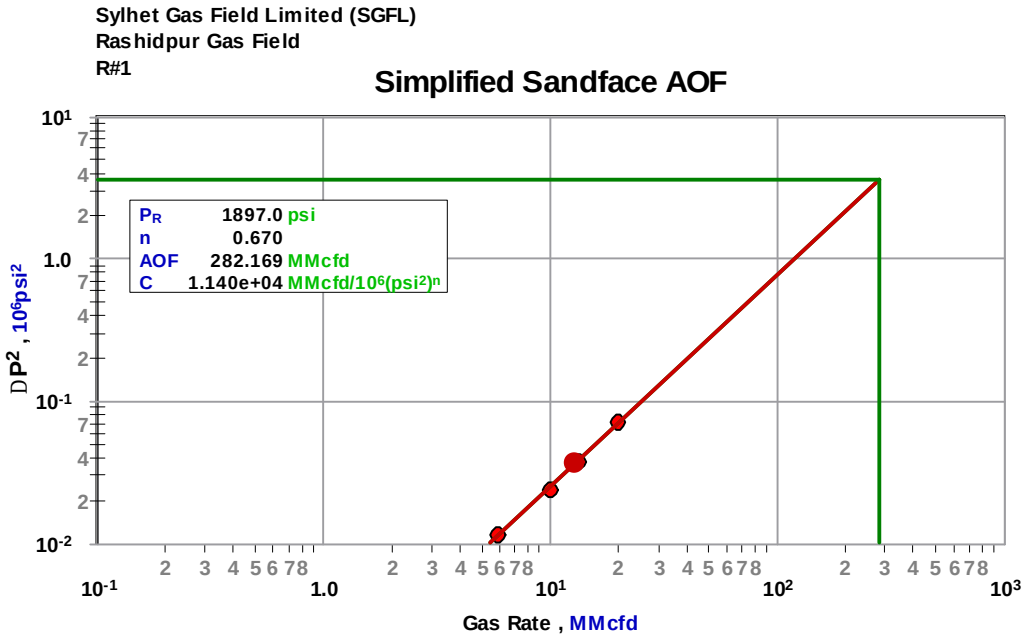

Figure 5.11: Deliverability line of R # 1

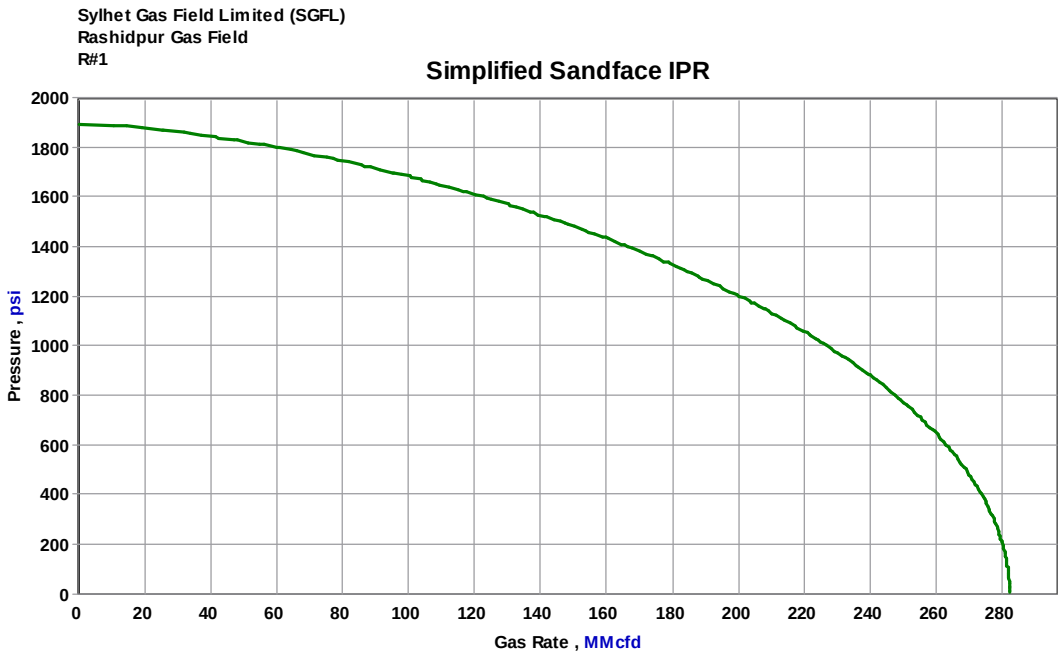

Figure 5.12: IPR curve of R # 1

Absolute Open Flow (AOF) Test Review

The major parameters that are found in Back Pressure Test are AOF=282.17 MMcfd, n=0.670 and C=1.14e+04 MMcfd/10 ^{6} $(psi^2)^n$.

5.3b R # 4

Here, 3 draw down data, (0.258 MMscfd, 2617 psia), (0.434 MMscfd, 2544psia) and (0.561 MMscfd, 2466 psia), are used to find out absolute open flow (AOF) potential. Shut-in pressure P_{WS}, 2758.5, found by buildup analysis, is taken as P_R. Extended flow data should have measured during the test. Hence, IPR/deliverability curve dose not represent the correct AOF and C. But value of n is not affected by this as the slope of the line is indicated by 1/n.

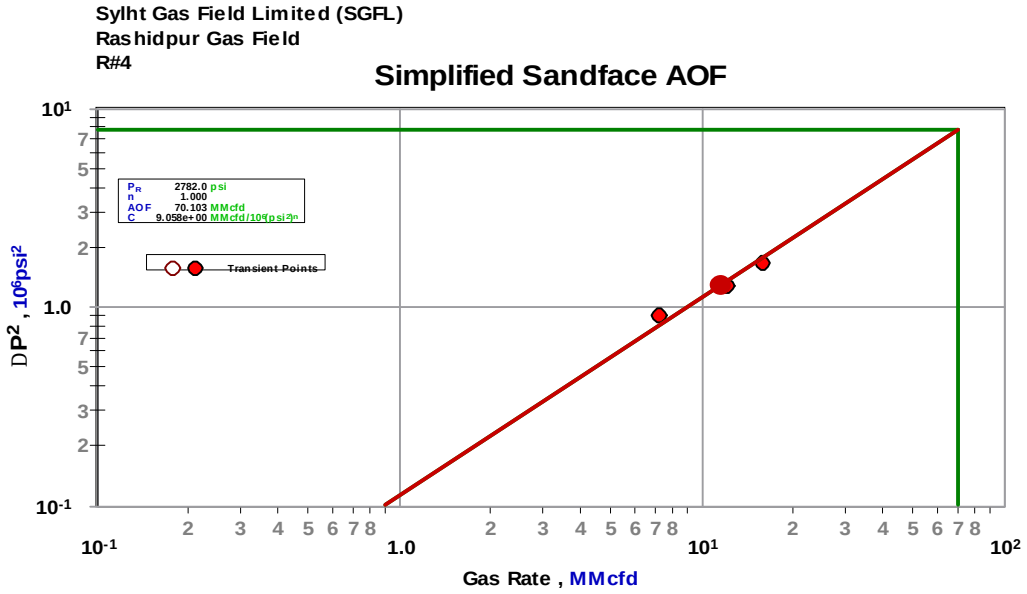

Figure 5.13: Deliverability line of R # 4

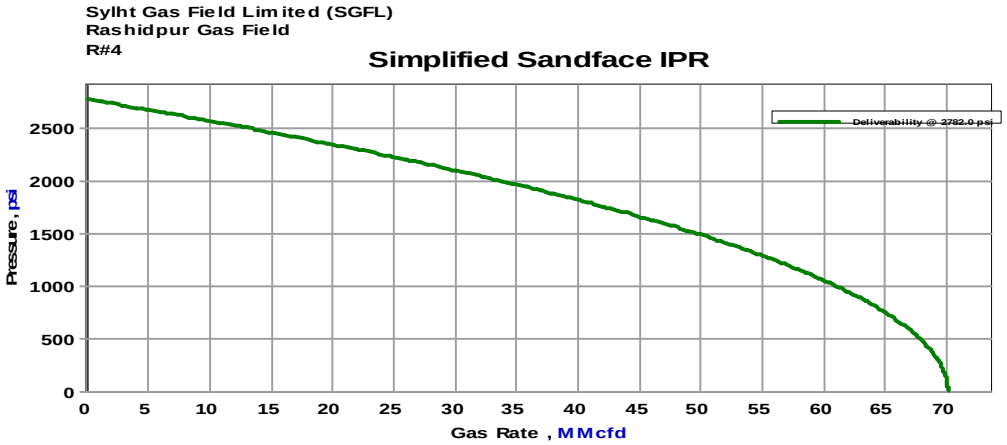

Figure 5.14: IPR curve of R # 4

Absolute Open Flow (AOF) Test Review

The major parameters that are found in Back Pressure Test are AOF=70.14 MMcfd, n=1.00 and C=2.39e-01 MMcfd/10 ^{6} $(psi^{2})^{n}$.

5.3c R # 7

Here, 3 draw down data, (7.137 MMscfd, 2237psia), (9.303 MMscfd, 2110 psia) and (10.704 MMscfd, 2043.8 psia), are used to find out absolute open flow (AOF) potential. . Shut-in pressure P_{WS}, 2610.7, found by buildup analysis, is taken as P_R. Extended flow data should have measured during the test. Hence, IPR/deliverability curve dose not represent the correct AOF and C. But value of n is not affected by this as the slope of the line is indicated by 1/n.

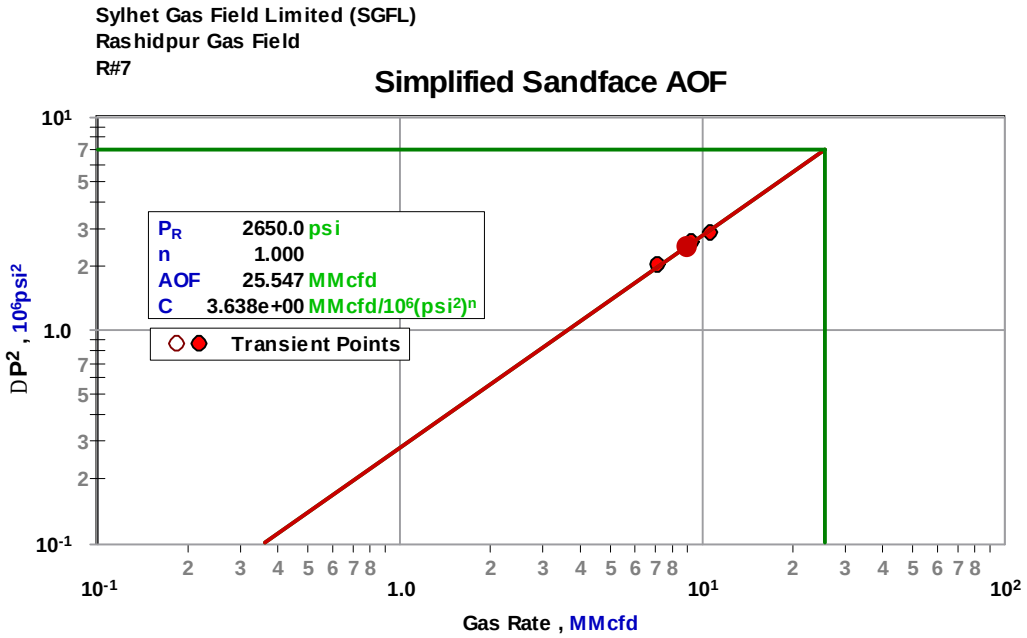

Figure 5.15: Deliverability line of R # 7

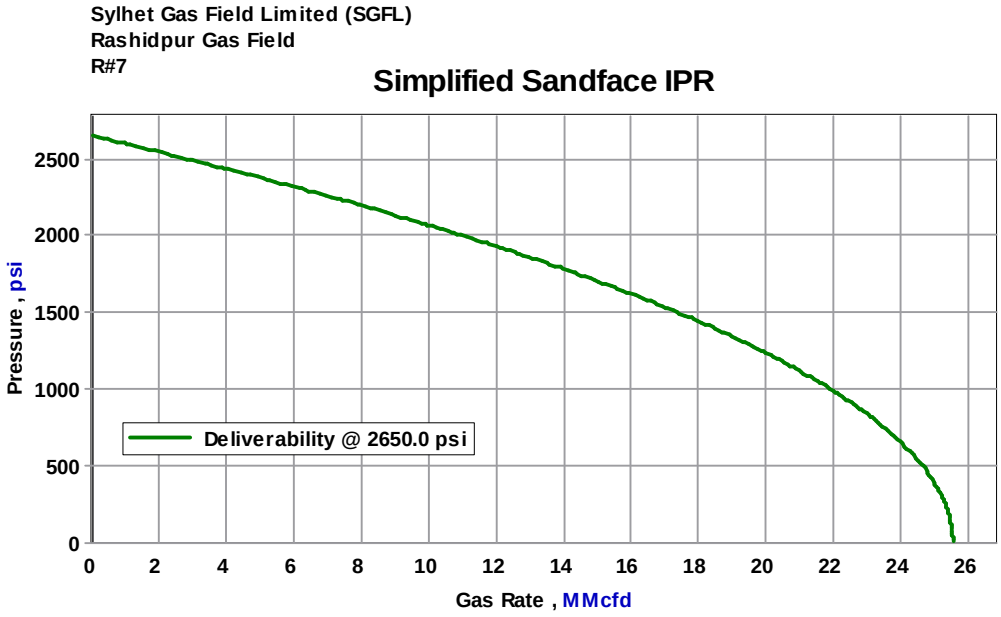

Figure 5.16: IPR curve of R # 7

Absolute Open Flow (AOF) Test Review

The major parameters that are found in Back Pressure Test are AOF=25.547 MMcfd, n=1.00 and C=3.638e+00 MMcfd/10 ^{6} $(psi^2)^n$

Table 5.1: Values of AOF (MMcfd), Constant, C and Exponent, n for different wells.

Name of Gas Field	Well	AOF (MMcfd)		Constant, C (MMcfd/10 ^{6} $(psi^2)^n$)		Exponent, n	
		Author of This Report	Almansoori	Author of This Report	Almansoori	Author of This Report	Almansoori
Kailastilla Gas Field	KTL#1	**537.12**	852.2	**4.38e+01**	4.86 **e** -05	**1.00**	1.15
	KTL#2	**1354.92**	3575	**1.811e+0**	0.799	**1.00**	0.638
	KTL#4	**358.6**	2490	**2.44e+02**	0.103	**0.870**	0.72
Biany Bazar Gas Field	BB#1	**52.69**	50.04	**4.437e+01**	1.45 **e-07**	**0.829**	1.16
	BB#2	**132.136**	251.0	**5.49e+01**	2.15 **e-07**	**0.872**	0.89
Rasidpur Gas Field	R#1	**282.17**	65.5	**1.14e+04**	189.8	**0.670**	0.29
	R#4	**70.14**	115	**2.39e-01**	2.32.**e-04**	**1.00**	1.266
	R#7	**25.547**	26.2	**3.638e+00**	2.12.**e-04**	**1.00**	0.92

Table 5.1 shows the values of AOF, Constant, C and Exponent, n for 8 different wells, whose are taken for analysis through this project work and IKM. From the results of Table 5.1, AOF value of KTL#2, followed by KTL#1, is very high but it is erroneous as flow rates was not accurate. R# 4 and R# 7 show a very low AOF value, maximum value (1.00) for Exponent, n, and negative skin (Table 4.13, Table 4.14). Low value of permeability and AOF indicates tight reservoir whereas maximum value (1.00) for Exponent, n, and negative skin indicates improved wellbore condition. Though same data, except computer software, are used by two analysts, results generated from two independent analysts for some wells, except BB#1, R#4 and R#7, vary widely.

CHAPTER 6

Conclusion and recommendation

6.1 Conclusion

Following conclusions can be drawn through the analysis of pressure transient data, for KTL#1, KTL#2 and KTL#4 of Kailashtilla Gas Field BB#1 and BB#2 of Biany Bazar Gas Field and, R#1, R#4 and R#7 of Rashidpur Gas Field .

Kailashtilla Gas Field

The findings, Total Permeability-thickness Product, kh (md. ft), Average permeability, K (md), Initial Reservoir Pressure, Pi (Psia), WellboreStorage Coefficient, C (bbl/psi) and Skin, S, of KTL#1, KTL#2 and KTL#4 of Kailashtilla Gas Field are shown in Table 4.3, Table 4.4 and Table 4.5 respectively. From core data analysis; Average Permeability of the Middle Gas Sand, producing zone of KTL#1 and KTL#4, is 88.4 md, and 424.3 md for the Upper Gas Sand, producing zone of KTL#2. Diagnosis results of KTL#1 and KTL#4 show a reasonable degree of deviation with geological evidence. Besides, KTL#2 shows very high permeability due to the exaggeration of gas flow rate.

Deliverability test results, AOF, (MMcfd), Exponent, n, and Coefficient, C, of KTL#1, KTL#2 and KTL#4 of Kailashtilla Gas Field along with the findings of Almansoori are shown in Table 5.1. Deliverability test results of KTL#2 are erroneous. AOF value of KTL#1 is very high whereas KTL#4 shows a reasonable AOF value. Maximum value (1.0) for Exponent, n, and low value (2.4) for skin of KTL#1 indicate a little damage in wellbore condition.

Biany Bazar Gas Field

The findings, Total Permeability-thickness Product, kh (md. ft), Average permeability, K (md), Initial Reservoir Pressure, Pi (Psia), WellboreStorage Coefficient, C (bbl/psi) and Skin, S, of BB#1 and BB#2 of Biany Bazar Gas Field are shown in Table 4.8 and Table 4.9 respectively. From core data analysis; Average Permeability of the Lower Gas Sand, producing zone of BB#1 is 189.6 md, and 332.4 md for the Upper Gas Sand, producing zone of BB#2. Diagnosis results of BB#1 and BB#2 show a large degree of deviation with geological evidence. Formation of condensate Bank near wellbore zone may be responsible for this deviation.

Deliverability test results, AOF, (MMcfd), Exponent, n, and Coefficient, C, of BB#1 and BB#2 of Biany Bazar Gas Field along with the findings of Almansoori are shown in Table 5.1. Deliverability test results, except Coefficient, C, show a rational difference between two analysts.

Rashidpur Gas Field

The findings, Total Permeability-thickness Product, kh (md. ft), Average permeability, K (md), Initial Reservoir Pressure, Pi (Psia), WellboreStorage Coefficient, C (bbl/psi) and Skin, S, of R# 1, R# 4 and R# 7 of Rashidpur Gas Field are shown in Table 4.12, Table 4.13 and Table 4.14 respectively. From core data analysis; Average Permeability of the Upper Gas Sand, producing zone of R#1, R#4 and R#7 is 370.0 md. Diagnosis results of R# 1, R# 4 and R# 7 show a high degree of deviation with geological evidence. Besides, very high permeability of R# 1 and a sudden upward trend (+1/2 slope line) for the pressure derivative indicates that the well might be within a channel.

Deliverability test results, AOF, (MMcfd), Exponent, n, and Coefficient, C, of R# 1, R# 4 and R# 7of Rashidpur Gas Field along with the findings of Almansoori are shown in Table 5.1. R# 4 and R# 7 show a very low AOF value, maximum value (1.00) for Exponent, n, and negative skin. Low value of permeability and AOF indicates tight reservoir whereas maximum value (1.00) for Exponent, n, and negative skin indicates improved wellbore condition.

6.2 Recommendation

Following recommendations can be drawn

1. Flow rate of gas, produced from KTL#1, KTL#2, KTL#3 and KTL#4, process by Molecular Sieve Turbo Expander (MSTE) plant in Kailashtilla Gas Field, must be measured separately in future well test, to nullify mixing effect.

2. Relevant data for two phase flow should be collected for future analysis as reservoirs in Kailashtilla and Byani Bazar Gas Field flow at high condensate gas ratio, which suggest a possibility of multi phase fluid flow in the reservoir.

3. Bottom hole position of well i.e. bottom hole co-ordinate of each well, which is diagnosis in chapter four, is very important parameter in model analysis to match synthetic pressure and pressure derivative actual data plot. Through the analysis in chapter four bottom hole co-ordinate of well is assumed. The author strongly recommends to use actual bottom hole co-ordinate of well, which is easily find out from well completion data or other sources, during future analysis.

4. In Back Pressure test only transient deliverability line is drawn through isochronal points. Normally an isochronal test includes one flow rate that is extended to stabilization and a stabilized pressure-flow rate point is determined. This point is the extended pressure and rate for the test. Hence in next time extended flow period pressure and rate have to collect to draw stabilized deliverability line parallel to transient deliverability line.

REFERENCES

American Society of Mechanical Engineers. ASME Transactions, Vol. 66, November 1944.

Bear, J. (1972). Dynamics of Fluids in Porous Media, Amer. Elsevier Publishing Co. ,Inc. , New York.

Beggs H. D.:"Gas Production Operations," OGCI., Tulsa 1984.

Carslaw, H. S. and J. C. Jaeger (1959). Conduction of Heat in Solids, Oxford Univ Press, London.

Earlougher, R. C., Jr.: "Advances in Well Test Analysis", Society of Petroleum Engineers Monograph 5, Dallas, TX, (1977).

ERCB. Theory and Practice of the testing of Gas Wells, 3-ed. Calgary: Energy Resources Conservation Board, 1975.

Cullender, M.H.: "The Isochronal Performance Method of Determining the Flow Characteristics of Gas Wells,"JPT, (July 1953) 137-142.

HAGOORT, J.:"Fundamentals of gas reservoir engineering," ELSEVER SCIENCE PUBLSHERS B. V. (1988).

Hong, K.C.:"Productivity of Perforated Completions in Formations With or Without Damage," J. Pet. Tech. (Aug. 1975) 1027-38; Trans., AIME, 259.

Horner,D. R. (1951). Pressure Build-up in Wells, Proceedings, Third World Pet. Congress-Sect. 2, 503-521.

Horne, R.N.:"Modern Well Test Analysis A Computer-Aided Approach," Petroway, Inc. (1995).

Houpert, A.:"On the Flow of Gases in Porous Media," Revue de L'Institut Francais du Petrole (1959) XIV (11), 1468-1684.

IKM- Page-29, Gas Field Appraisal Project Geological, Geophysical and Petrophysical Report Kailashtilla Gas Field Bangladesh, July, 1989

Ikoku, Chi U. "Natural Gas Reservoir Engineering" pp-170-172,1992.

Katz, D.L., et al.:"Handbook of Natural Gas Engineering," McGraw Hill Book Co.,Inc., New York 1959.

Lee, A. L., Gonzalez , M. H., and Eakin, B. E.:"The Viscosity of Natural Gases," J. Pet. Tech. (Aug., 1966).

Lock, S.:" An Advanced Method for Predicting The Productivity Ratio of A perforated Well, "J. Pet. Tech. (Dec. 1981) 2481 – 2488.

Mattthew, C.S., Brons, F., and Hazebroek, P.: "A Method for Determination of Average Reservoir Pressurein Bounded Reservoirs", Trans., AIME, (1954), 201, 182-191.

Ramey, H. J., Jr. and W. M. Cobb (1971). A General Pressure Buildup Theory for a Well in a Closed Drainage Area, J. Pet. Tech., 23, 1493-1505.

Rawlins, E.L., and M.A. Schellhardt (1936). Back pressure data Natural Gas wells and their application to production practices, U. S. Bureau of minees, monograph 7, U.S Bureau of Mines (1936).

Theory and practice of the testing of gas wells third edition, 1975,Enetrgy resources conservation Board, Calgary, Alberta, Canada.
SGFL Annual Report 2006-07.

Theis, C.V. (1935) The relation Between the Lowering of the Piezometric Surface and the Rate and Duration of Discharge of a Well Using Ground Water Storage, Amer. Geophys. Union Trans. ,16, 519-524.

APPENDIX A

Reservoir and well related data essential for analysis

Parameters	KTL#1	KTL#2	KTL#4	BB#1	BB#2	R#1	R#4	R#7
Well Radius (inches)	4	3.5	3.5	4	4	4	3.5	3.5
Net Drained Thickness (ft)	65	40	69	20	52	142	40	26
Interval tested (ft)	9652'-9655', 9658'-9664', 9668'-9722'	7390'-7430'	9610'-9673' 9696'-9702'	11350'-11370'	10774' – 10826'	4596'-4651', 4661-4741', 4802'-4809'	9144' -9164', 9180' - 9200	9123' -9149'
Effective Porosity (%)	0.16 (assumed value)	0.16 (assumed value)	0.10 (assumed value)	0.16	0.20	0.25	0.18 (assumed value)	0.13
Gas Gravity	0.59	0.586	0.586	0.596	0.596	0.565	0.582	0.565
Condensate Gravity 'API								
Condensate Gas Ratio (stb/MMscf)								
Primary Separator Pressure (Psia)	1000	1000	1000	1000	1000	1000	1000	1000
Primary Separator Temp ('F)	70	70	70	70	70	70	70	70
Dew Point	not available	not available	not available	not available	not available	not available	not available	not available
CO2 Component (mol %)	0.142	0.139	0.1432	0.090	0.090	0.179	0.179	0.179
H2S Component (mol %)	Nil	Nil	Nil	Nil	Nil	Nil	Nil	Nil
N2 Component (mol %)	Nil	Nil	Nil	0.38	0.38	0.3977	0.3977	0.3977
Water Salinity (ppm)	10000 (Assumed value)	10000 (Assumed value)	10000 (Assumed value)	175000 (Assumed value)	150000 (Assumed value)	10000 (Assumed value)	10000 (Assumed value)	10000 (Assumed value)
Initial Reservoir Pressure (Psia)	3515 (From PTA)	3221 (From PTA)	3491 (From PTA)	4849	4898	2051	2771 (From PTA)	2621 (From PTA)
Initial Reservoir Temp ('F)	166.3	145.11	162.7	202	198	113	155	148
Rock Compressibility (psi^{-1})	not available	not available	not available	not available	not available	not available	not available	not available
WGR bbl/MMscf							0.95	
Connate water saturation (%)	36	15	36	21	20	30-35	30-35	20